

FINITE DATA PERFORMANCE ANALYSIS OF LCMV ANTENNA ARRAY BEAMFORMERS WITH AND WITHOUT SIGNAL BLOCKING

Y.-L. Chen¹ and J.-H. Lee^{2, *}

¹Graduate Institute of Communication Engineering, National Taiwan University, No. 1, Sec. 4, Roosevelt Rd., Taipei 10617, Taiwan

²Department of Electrical Engineering, Graduate Institute of Communication Engineering, and Graduate Institute of Biomedical Electronics and Bioinformatics, National Taiwan University, No. 1, Sec. 4, Roosevelt Rd., Taipei 10617, Taiwan

Abstract—A linearly constrained minimum variance (LCMV) antenna array beamformer using finite data samples suffers from slow convergence when the received array data contain the desired signal. It has been reported that signal blocking techniques speed up the convergence rate and increase the robustness of LCMV antenna array beamformers. However, the reason of this improvement has not been explored in the literature. Moreover, the existing formulas for the output signal-to-interference-plus-noise ratio (SINR) are too rough to realize the influence of signal blocking techniques on the performance. In this paper, we show that the correlation due to finite samples causes the redundant component (termed as the cross weight) embedded in the weight vector of a LCMV beamformer even if the signal sources and noise are independent. The cross power results from the cross weight degrades the performance when the sample size is small. In contrast, the cross weight and cross power can be fully eliminated when a signal blocking technique is used. The theoretical results presented in this paper provide a comprehensive description on the effectiveness and the price of using signal blocking for antenna array beamforming. Simulation results are also given for confirming the validity of the theoretical results.

Received 4 May 2012, Accepted 6 July 2012, Scheduled 17 August 2012

* Corresponding author: J.-H. Lee (juhong@cc.ee.ntu.edu.tw).

1. INTRODUCTION

For an antenna array beamformer, several practical situations degrade its performance. Among them, the finite sample effect is frequently considered. This effect comes from the fact that the ensemble data correlation matrix is usually unknown and is estimated by taking finite data samples. In the literature, the finite data performance of a linearly constrained minimum variance (LCMV) beamformer has been analyzed in [1–3]. Wax and Anu [1] gave detail discussions for the behavior of a LCMV beamformer under several special cases. Chang and Yeh [2] derived the output signal-to-interference-plus-noise ratio (SINR) of a LCMV beamformer under one desired signal and one interferer. Reed et al. [3] analyzed a LCMV beamformer without the desired signal in the received data. However, the existing results can not be directly extended to the case with one desired signal and multiple interferers.

The signal blocking technique was originally proposed by Widrow et al. [4] to tackle the coherent problem. Due to its effectiveness, the idea of removing the desired signal before computing the weights has been widely applied for antenna array beamforming [5–10]. Notable among them are [5, 8]. In [5], the authors proposed an eigencanceller constraining the weight vector to be orthogonal to the interference subspace instead of the conventional LCMV criteria. Later, a statistical analysis to this eigencanceller was presented in [8], where a compensation matrix was proposed for eliminating the blocking effect on the noise. It was shown that the eigencanceller can eliminate interference efficiently and has a fast convergence rate. Nevertheless, the signal blocking effect is still unknown in both [5] and [8].

Recently, an analysis of LCMV beamformers with and without signal blocking under pointing error and finite sample effect was presented in [11]. The derivations are based on the probability density function of the weight vector given by [12, 13]. The formulas presented in [11] demonstrate the drawback of the one dimension loss when signal blocking is used. Although the analysis in [11] provides accurate formulas to describe the output SINRs, the robustness enhancement and convergence rate improvement for signal blocking is, however, invisible either from the derivations or the final theoretical results. In addition, the effects of system parameters such as source directions, signal powers, or array configurations on the output SINRs are still unknown from the expressions.

In this paper, we consider the performance of LCMV beamformers with and without signal blocking under finite samples and derive the output SINR formulas for the LCMV beamformers with and without

signal blocking. Based on the theoretical results, the merits and defects of using a signal blocking technique can be described comprehensively. Besides, these theoretical results can be easily extended to the case with multiple interferers. Simulation results confirm the accuracy of the theoretical results.

This paper is organized as follows. Section 2 briefly describes the principles of LCMV beamformers with and without signal blocking. In Section 3 and Section 4, we analyze the performances of a LCMV beamformer without and with signal blocking, respectively. Simulation results are presented in Section 5 for confirming the validity of the research work. Finally, we make a conclusion in Section 6.

2. PRINCIPLES OF LCMV BEAMFORMERS

2.1. A LCMV Beamformer without Signal Blocking

Let q independent narrowband signal sources including one desired signal and $(q - 1)$ interferers impinge on a conventional LCMV beamformer with p array sensors, $q < p$. The data vector received by the array beamformer can be expressed as

$$\mathbf{x}(t) = s_1(t) \mathbf{a}_1 + \sum_{k=2}^q s_k(t) \mathbf{a}_k + \mathbf{n}(t) = s_1(t) \mathbf{a}_1 + \mathbf{v}(t), \quad (1)$$

where $s_i(t)$ is the complex waveform of the i th signal source with zero mean and variance $\sigma_{s_i}^2$; \mathbf{a}_i is the corresponding steering vector, $i = 1, 2, \dots, q$; $\mathbf{v}(t)$ is the undesired component including the interference and noise. $\mathbf{n}(t)$ denotes the noise vector with zero mean and variance σ_n^2 and is independent of the q signal sources. The ensemble correlation matrix of $\mathbf{x}(t)$ is given by

$$\mathbf{R} = E [\mathbf{x}(t) \mathbf{x}^H(t)] = \sigma_{s_1}^2 \mathbf{a}_1 \mathbf{a}_1^H + \mathbf{Q}, \quad (2)$$

where the superscript “ H ” denotes the conjugate and transpose operation. \mathbf{Q} is given by

$$\mathbf{Q} = E [\mathbf{v}(t) \mathbf{v}^H(t)] = \sum_{k=2}^q \sigma_{s_k}^2 \mathbf{a}_k \mathbf{a}_k^H + \sigma_n^2 \mathbf{I}, \quad (3)$$

and \mathbf{I} is the identity matrix with appropriate size. The weight vector of the LCMV beamformer can be obtained by solving the following optimization problem [14, 15]:

$$\text{Minimize } \mathbf{w}^H \mathbf{R} \mathbf{w} \quad \text{Subject to } \mathbf{w}^H \mathbf{a}_1 = 1. \quad (4)$$

The solution of (4) is given by [14, 15]

$$\mathbf{w}_o = \frac{\mathbf{R}^{-1}\mathbf{a}_1}{\mathbf{a}_1^H\mathbf{R}^{-1}\mathbf{a}_1} = \frac{\mathbf{Q}^{-1}\mathbf{a}_1}{\mathbf{a}_1^H\mathbf{Q}^{-1}\mathbf{a}_1}. \quad (5)$$

However, the ensemble correlation matrix \mathbf{R} is not available in practice. Its approximation computed by taking data samples is given as follows [3, 16]:

$$\hat{\mathbf{R}} = \frac{1}{m} \sum_{i=1}^m \mathbf{x}(t_i) \mathbf{x}^H(t_i), \quad (6)$$

where $\mathbf{x}(t_i)$ denotes the i th data sample of $\mathbf{x}(t)$ taken at the i th time instant, $i = 1, 2, \dots, m$. Hence, the solution of (5) becomes

$$\hat{\mathbf{w}} = \frac{\hat{\mathbf{R}}^{-1}\mathbf{a}_1}{\mathbf{a}_1^H\hat{\mathbf{R}}^{-1}\mathbf{a}_1}. \quad (7)$$

According to the result of [1], the sample correlation matrix $\hat{\mathbf{R}}$ can be expressed as follows:

$$\hat{\mathbf{R}} = \hat{\sigma}_{s_1}^2 \mathbf{a}_1 \mathbf{a}_1^H + \mathbf{a}_1 \hat{\mathbf{r}}^H + \hat{\mathbf{r}} \mathbf{a}_1^H + \hat{\mathbf{Q}}, \quad (8)$$

where $\hat{\sigma}_{s_1}^2 = (1/m) \sum_{i=1}^m |s_1(t_i)|^2$, $\hat{\mathbf{Q}} = (1/m) \sum_{i=1}^m \mathbf{v}(t_i) \mathbf{v}^H(t_i)$, and $\hat{\mathbf{r}} = (1/m) \sum_{i=1}^m s_1^*(t_i) \mathbf{v}(t_i)$ are the sample mean of the desired signal power, the sample version of \mathbf{Q} , and the sample version of the cross correlation between the desired signal and the undesired component, respectively. Since the signal sources and noise are mutually independent, we have

$$E[\hat{\mathbf{r}}] = \frac{1}{m} \sum_{i=1}^m E[s_1^*(t_i)] E[\mathbf{v}(t_i)] = \mathbf{0}. \quad (9)$$

2.2. A LCMV Beamformer with Signal Blocking

Figure 1 depicts a LCMV beamformer with signal blocking. The signal blocking matrix \mathbf{B} is employed to block the desired signal with the presumed look direction \mathbf{a}_1 , i.e., [6, 17]

$$\mathbf{B}\mathbf{a}_1 = \mathbf{0}. \quad (10)$$

Let the data vector after the blocking operation be $\mathbf{x}_B(t_i) = \mathbf{B}\mathbf{x}(t_i)$ and \mathbf{B} be of size $N \times p$ with $N < p$. The $N \times 1$ weight vector required for beamforming is given by [6, 7]

$$\hat{\mathbf{w}}_B = \frac{\hat{\mathbf{R}}_B^{-1}\mathbf{a}_1}{\mathbf{a}_1^H\hat{\mathbf{R}}_B^{-1}\mathbf{a}_1}, \quad (11)$$

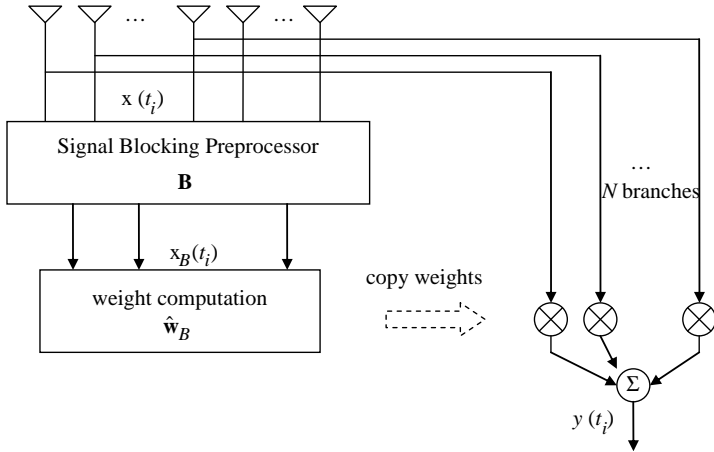


Figure 1. A LCMV beamformer with signal blocking.

where $\hat{\mathbf{R}}_B$ is the $N \times N$ sample correlation matrix of $\mathbf{x}_B(t)$ and given by $\hat{\mathbf{R}}_B = \mathbf{B}\hat{\mathbf{R}}\mathbf{B}^H$. Without loss of generality, we set $\bar{\mathbf{a}}_k$ to contain the first N entries of \mathbf{a}_k , $k=1, 2, \dots, q$. It follows from (8) that

$$\hat{\mathbf{R}}_B = \mathbf{B} \left(\hat{\sigma}_{s1}^2 \mathbf{a}_1 \mathbf{a}_1^H + \mathbf{a}_1 \hat{\mathbf{r}}^H + \hat{\mathbf{r}} \mathbf{a}_1^H + \hat{\mathbf{Q}} \right) \mathbf{B}^H = \mathbf{B} \hat{\mathbf{Q}} \mathbf{B}^H. \quad (12)$$

Equation (12) reveals that the cross terms $\mathbf{a}_1 \hat{\mathbf{r}}^H$ and $\hat{\mathbf{r}} \mathbf{a}_1^H$ in $\hat{\mathbf{R}}$ due to finite samples are removed. Let $\hat{\mathbf{Q}}_B = \mathbf{B} \hat{\mathbf{Q}} \mathbf{B}^H$, (11) can be rewritten as

$$\hat{\mathbf{w}}_B = \frac{\hat{\mathbf{Q}}_B^{-1} \bar{\mathbf{a}}_1}{\bar{\mathbf{a}}_1^H \hat{\mathbf{Q}}_B^{-1} \bar{\mathbf{a}}_1}. \quad (13)$$

2.3. The Existing Analysis Results

In [11], the array output SINRs based on $\hat{\mathbf{w}}$ and $\hat{\mathbf{w}}_B$ were derived to

$$SINR_L = \frac{\sigma_{s1}^2 \mathbf{a}_1^H \mathbf{R}^{-1} \mathbf{a}_1}{\frac{\text{tr}(\mathbf{Q}\mathbf{R}^{-1})}{m-p+1} + \frac{m-p}{m-p+1} \cdot \frac{\mathbf{a}_1^H \mathbf{R}^{-1} \mathbf{Q} \mathbf{R}^{-1} \mathbf{a}_1}{\mathbf{a}_1^H \mathbf{R}^{-1} \mathbf{a}_1}} \quad (14)$$

and

$$SINR_B = \frac{\sigma_{s1}^2 \bar{\mathbf{a}}_1^H \mathbf{R}_B^{-1} \bar{\mathbf{a}}_1}{\frac{\text{tr}(\bar{\mathbf{Q}}\mathbf{R}_B^{-1})}{m-p+2} + \frac{m-p+1}{m-p+2} \cdot \frac{\bar{\mathbf{a}}_1^H \mathbf{R}_B^{-1} \bar{\mathbf{Q}} \mathbf{R}_B^{-1} \bar{\mathbf{a}}_1}{\bar{\mathbf{a}}_1^H \mathbf{R}_B^{-1} \bar{\mathbf{a}}_1}}, \quad (15)$$

respectively, where $\bar{\mathbf{Q}}$ is obtained by removing the p th row and column of \mathbf{Q} , and $\mathbf{R}_B = \mathbf{B}\mathbf{R}\mathbf{B}^H$ is the ensemble version of $\hat{\mathbf{R}}_B$. Although (14)

and (15) were derived without making approximations, it is not easy to observe the pros and cons of signal blocking from (14) and (15). In addition, the effects of system parameters such as source directions, signal powers, or array configurations on the output SINRs can not be observed directly from (14) and (15).

3. PERFORMANCE OF A LCMV BEAMFORMER WITHOUT SIGNAL BLOCKING

Under finite data samples, the output of a LCMV beamformer is given by $y(t) = \hat{\mathbf{w}}^H \mathbf{x}(t)$. Using (1), (2), and (3), we have

$$\begin{aligned} E[|y(t)|^2] &= E\left[\sigma_{s1}^2 |\hat{\mathbf{w}}^H \mathbf{a}_1|^2\right] + E\left[\sum_{k=2}^q \sigma_{sk}^2 |\hat{\mathbf{w}}^H \mathbf{a}_k|^2\right] + E[\sigma_n^2 \hat{\mathbf{w}}^H \hat{\mathbf{w}}] \\ &\equiv P_s + P_i + P_n. \end{aligned} \quad (16)$$

From (7) and (16), the output SINR of a LCMV beamformer without signal blocking is given by

$$\begin{aligned} SINR_L &= \frac{P_s}{P_i + P_n} = \frac{E\left[\sigma_{s1}^2 |\hat{\mathbf{w}}^H \mathbf{a}_1|^2\right]}{E\left[\sum_{k=2}^q \sigma_{sk}^2 |\hat{\mathbf{w}}^H \mathbf{a}_k|^2\right] + E[\sigma_n^2 \hat{\mathbf{w}}^H \hat{\mathbf{w}}]} \\ &= \frac{\sigma_{s1}^2}{E\left[\sum_{k=2}^q \sigma_{sk}^2 |\hat{\mathbf{w}}^H \mathbf{a}_k|^2\right] + E[\sigma_n^2 \hat{\mathbf{w}}^H \hat{\mathbf{w}}]}. \end{aligned} \quad (17)$$

The weight vector of $\hat{\mathbf{w}}$ in (7) can be derived to [1, Eq. (20)]

$$\hat{\mathbf{w}} = \frac{\hat{\mathbf{Q}}^{-1} \mathbf{a}_1}{\mathbf{a}_1^H \hat{\mathbf{Q}}^{-1} \mathbf{a}_1} - \hat{\mathbf{P}} \hat{\mathbf{Q}}^{-1} \hat{\mathbf{r}}, \quad (18)$$

where $\hat{\mathbf{P}} = \mathbf{I} - \hat{\mathbf{Q}}^{-1} \mathbf{a}_1 \mathbf{a}_1^H / \mathbf{a}_1^H \hat{\mathbf{Q}}^{-1} \mathbf{a}_1$. The first term in (18) $\hat{\mathbf{w}}_Q \equiv \hat{\mathbf{Q}}^{-1} \mathbf{a}_1 / \mathbf{a}_1^H \hat{\mathbf{Q}}^{-1} \mathbf{a}_1$ represents the weight vector without the desired signal in the received data vector. The second term is related to the cross correlation $\hat{\mathbf{r}}$ between the desired signal and undesired component. According to the analysis in [3], the difference between the output SINRs of using $\hat{\mathbf{w}}_Q$ and the optimal \mathbf{w}_o is within 3 dB when the number m of data samples is larger than twice of the number of array elements. Then, Anu and Wax [1] extended this result and claimed that the $\hat{\mathbf{r}}$ in (18) captures the most finite sample effect as compared with the other random quantities $\hat{\mathbf{Q}}$ and $\hat{\mathbf{P}}$. For a moderate sample

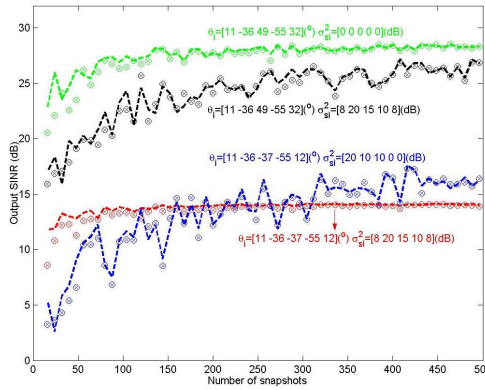


Figure 2. Output SINRs computed by three weight vectors. ‘o’: the LCMV weight vector in (7). ‘x’: the weight vector in (18). ‘-’: the approximated weight vector in (19).

size $m > 3p$, it is also shown in [1, Eq. (21)] that $\hat{\mathbf{w}}$ in (18) can be approximated by

$$\hat{\mathbf{w}} \approx \frac{\mathbf{Q}^{-1}\mathbf{a}_1}{\mathbf{a}_1^H\mathbf{Q}^{-1}\mathbf{a}_1} - \mathbf{P}\mathbf{Q}^{-1}\hat{\mathbf{r}} = \mathbf{w}_o + \hat{\mathbf{w}}_c, \tag{19}$$

where

$$\mathbf{P} = \mathbf{I} - \frac{\mathbf{Q}^{-1}\mathbf{a}_1\mathbf{a}_1^H}{\mathbf{a}_1^H\mathbf{Q}^{-1}\mathbf{a}_1} \quad \text{and} \quad \hat{\mathbf{w}}_c = -\mathbf{P}\mathbf{Q}^{-1}\hat{\mathbf{r}}. \tag{20}$$

A trial with four parameter settings for the output SINRs computed by (7), (18), and (19) are presented in Figure 2 for an eight-element uniform linear array (ULA) with half-wavelength spacing. We observe that the approximation used in (19) results in acceptable errors and still preserves the most finite sample effect even if the output SINRs have not reached the steady-state (i.e., optimal SINR). To facilitate the following analysis, we adopt this approximation. Equation (19) shows that a redundant component $\hat{\mathbf{w}}_c$ called cross weight is produced when the finite sample effect exists.

3.1. Output SINR in Terms of Q

Substituting (19) into the term P_i of (17) yields

$$P_i = E \left[\sum_{k=2}^q \sigma_{sk}^2 |\hat{\mathbf{w}}^H \mathbf{a}_k|^2 \right]$$

$$\begin{aligned} &\approx \sum_{k=2}^q \sigma_{sk}^2 |\mathbf{w}_o^H \mathbf{a}_k|^2 + \sum_{k=2}^q \sigma_{sk}^2 E[\hat{\mathbf{w}}_c] \mathbf{a}_k \mathbf{a}_k^H \mathbf{w}_o \\ &\quad + \sum_{k=2}^q \sigma_{sk}^2 \mathbf{w}_o^H \mathbf{a}_k \mathbf{a}_k^H E[\hat{\mathbf{w}}_c] + \sum_{k=2}^q \sigma_{sk}^2 E[|\hat{\mathbf{w}}_c^H \mathbf{a}_k|^2]. \end{aligned} \quad (21)$$

Using (9) and (20), we have $E[\hat{\mathbf{w}}_c] = \mathbf{0}$ and

$$P_i \approx \sum_{k=2}^q \sigma_{sk}^2 |\mathbf{w}_o^H \mathbf{a}_k|^2 + \sum_{k=2}^q \sigma_{sk}^2 E[|\hat{\mathbf{w}}_c^H \mathbf{a}_k|^2] \equiv P_{io} + P_{ic}. \quad (22)$$

Then, substituting \mathbf{w}_o of (5) and $\hat{\mathbf{w}}_c$ of (20) into (22) yields the optimal interference output power and the additional interference output power due to finite samples as follows:

$$P_{io} = \sum_{k=2}^q \sigma_{sk}^2 \left| \frac{\mathbf{a}_1^H \mathbf{Q}^{-1} \mathbf{a}_k}{\mathbf{a}_1^H \mathbf{Q}^{-1} \mathbf{a}_1} \right|^2 \quad (23)$$

and

$$P_{ic} = \sum_{k=2}^q \sigma_{sk}^2 E[|\hat{\mathbf{r}}^H \mathbf{Q}^{-1} \mathbf{P}^H \mathbf{a}_k|^2] = \sum_{k=2}^q \sigma_{sk}^2 \mathbf{a}_k^H \mathbf{P} \mathbf{Q}^{-1} E[\hat{\mathbf{r}} \hat{\mathbf{r}}^H] \mathbf{Q}^{-1} \mathbf{P}^H \mathbf{a}_k, \quad (24)$$

respectively. Since

$$E[\hat{\mathbf{r}} \hat{\mathbf{r}}^H] = \frac{1}{m^2} \sum_{i=1}^m \sum_{k=1}^m E[s_1^*(t_i) \mathbf{v}(t_i) s_1(t_k) \mathbf{v}^H(t_k)] = \frac{\sigma_{s1}^2}{m} \mathbf{Q} \quad (25)$$

and $\mathbf{P} = \mathbf{I} - \mathbf{Q}^{-1} \mathbf{a}_1 \mathbf{a}_1^H / (\mathbf{a}_1^H \mathbf{Q}^{-1} \mathbf{a}_1)$, (24) becomes

$$P_{ic} = \frac{\sigma_{s1}^2}{m} \sum_{k=2}^q \sigma_{sk}^2 \left(\mathbf{a}_k^H \mathbf{Q}^{-1} \mathbf{a}_k - \frac{|\mathbf{a}_k^H \mathbf{Q}^{-1} \mathbf{a}_1|^2}{\mathbf{a}_1^H \mathbf{Q}^{-1} \mathbf{a}_1} \right). \quad (26)$$

Similarly, substituting (19) into the term P_n of (17) yields

$$P_n \approx \sigma_n^2 \mathbf{w}_o^H \mathbf{w}_o + \sigma_n^2 E[\hat{\mathbf{w}}_c^H \hat{\mathbf{w}}_c] \equiv P_{no} + P_{nc}. \quad (27)$$

Using \mathbf{w}_o of (5) and $\hat{\mathbf{w}}_c$ of (20), we obtain

$$P_{no} = \sigma_n^2 \frac{\|\mathbf{Q}^{-1} \mathbf{a}_1\|^2}{(\mathbf{a}_1^H \mathbf{Q}^{-1} \mathbf{a}_1)^2} \quad (28)$$

and

$$P_{nc} = \sigma_n^2 E[\hat{\mathbf{r}}^H \mathbf{Q}^{-1} \mathbf{P}^H \mathbf{P} \mathbf{Q}^{-1} \hat{\mathbf{r}}] = \sigma_n^2 \text{tr}(\mathbf{Q}^{-1} \mathbf{P}^H \mathbf{P} \mathbf{Q}^{-1} E[\hat{\mathbf{r}} \hat{\mathbf{r}}^H]), \quad (29)$$

where $\|\mathbf{x}\|^2$ denotes the squared norm of the vector \mathbf{x} and $tr(\mathbf{X})$ the trace of the matrix \mathbf{X} . From (25) and (20), we have P_{nc} given by

$$P_{nc} = \sigma_n^2 \frac{\sigma_{s1}^2}{m} \left(tr(\mathbf{Q}^{-1}) - \frac{\|\mathbf{Q}^{-1}\mathbf{a}_1\|^2}{\mathbf{a}_1^H \mathbf{Q}^{-1} \mathbf{a}_1} \right). \tag{30}$$

Using P_{ic} of (26) and P_{nc} of (30) and performing some algebraic manipulations yields the additional power in the denominator of (17) due to $\hat{\mathbf{w}}_c$ as follows:

$$P_c \equiv P_{ic} + P_{nc} = \frac{\sigma_{s1}^2}{m} (p - 1). \tag{31}$$

Since the cross weight produces a positive P_c (called cross power) in the denominator of (17), the effect of using finite data samples degrades the beamforming performance. From (22), (23), (27), (28), and (31), we can rewrite (17) as follows:

$$\begin{aligned} SINR_L &\approx \frac{\sigma_{s1}^2}{P_{io} + P_{no} + P_c} \\ &= \frac{\sigma_{s1}^2}{\sum_{k=2}^q \sigma_{sk}^2 \left| \frac{\mathbf{a}_1^H \mathbf{Q}^{-1} \mathbf{a}_k}{\mathbf{a}_1^H \mathbf{Q}^{-1} \mathbf{a}_1} \right|^2 + \sigma_n^2 \frac{\|\mathbf{Q}^{-1} \mathbf{a}_1\|^2}{(\mathbf{a}_1^H \mathbf{Q}^{-1} \mathbf{a}_1)^2} + \frac{(p-1)\sigma_{s1}^2}{m}}. \end{aligned} \tag{32}$$

3.2. Derivation of \mathbf{Q}^{-1}

Assume a set of dummy variables $\mathbf{K}_r, r = 1, 2, \dots, q$, defined as follows:

$$\mathbf{K}_r = \begin{cases} \sigma_n^2 \mathbf{I} & r = 1 \\ \sum_{i=2}^r \sigma_{si}^2 \mathbf{a}_i \mathbf{a}_i^H + \sigma_n^2 \mathbf{I} & 2 \leq r \leq q \end{cases}. \tag{33}$$

Hence, \mathbf{Q}^{-1} can be expressed as

$$\mathbf{Q}^{-1} = \mathbf{K}_q^{-1} = (\mathbf{K}_{q-1} + \sigma_{sq}^2 \mathbf{a}_q \mathbf{a}_q^H)^{-1}. \tag{34}$$

Applying the matrix inversion lemma to (34), we obtain the following recursive formula

$$\mathbf{Q}^{-1} = \mathbf{K}_q^{-1} = \mathbf{K}_{q-1}^{-1} \left(\mathbf{I} - \frac{\mathbf{a}_q \mathbf{a}_q^H \mathbf{K}_{q-1}^{-1}}{\sigma_{sq}^{-2} + \mathbf{a}_q^H \mathbf{K}_{q-1}^{-1} \mathbf{a}_q} \right) \tag{35}$$

with $\mathbf{K}_1^{-1} = \sigma_n^{-2} \mathbf{I}$. It follows from (35) that

$$\mathbf{Q}^{-1} = \underbrace{\underbrace{\underbrace{(\sigma_n^{-2} \mathbf{I}) \left(\mathbf{I} - \frac{\mathbf{a}_2 \mathbf{a}_2^H \mathbf{K}_1^{-1}}{\sigma_{s2}^{-2} + \mathbf{a}_2^H \mathbf{K}_1^{-1} \mathbf{a}_2} \right)}_{\mathbf{K}_1^{-1}}}_{\mathbf{K}_2^{-1}} \left(\mathbf{I} - \frac{\mathbf{a}_3 \mathbf{a}_3^H \mathbf{K}_2^{-1}}{\sigma_{s3}^{-2} + \mathbf{a}_3^H \mathbf{K}_2^{-1} \mathbf{a}_3} \right)}_{\mathbf{K}_3^{-1}}$$

$$\dots \left(\mathbf{I} - \frac{\mathbf{a}_q \mathbf{a}_q^H \mathbf{K}_{q-1}^{-1}}{\sigma_{sq}^{-2} + \mathbf{a}_q^H \mathbf{K}_{q-1}^{-1} \mathbf{a}_q} \right) = \sigma_n^{-2} \prod_{i=2}^q \left(\mathbf{I} - \frac{\mathbf{a}_i \mathbf{a}_i^H \mathbf{K}_{i-1}^{-1}}{\sigma_{si}^{-2} + \mathbf{a}_i^H \mathbf{K}_{i-1}^{-1} \mathbf{a}_i} \right). \quad (36)$$

Substituting (36) into (32) provides an explicit formula for computing $SINR_L$ under any q interferers. Moreover, the recursive formula shown by (36) facilitates the computation process.

3.3. Output SINR for Two Interferers

Substituting $q = 3$ into (36) and performing some algebraic manipulations yields

$$\mathbf{Q}^{-1} = \frac{\sigma_n^{-2} \left\{ \begin{array}{l} \sigma_n^4 \mathbf{I} + \sigma_{s2}^2 \sigma_n^2 [(\mathbf{a}_2^H \mathbf{a}_2) \cdot \mathbf{I} - \mathbf{a}_2 \mathbf{a}_2^H] + \sigma_{s3}^2 \sigma_n^2 [(\mathbf{a}_3^H \mathbf{a}_3) \cdot \mathbf{I} - \mathbf{a}_3 \mathbf{a}_3^H] \\ + \sigma_{s2}^2 \sigma_{s3}^2 \left[(\mathbf{a}_2^H \mathbf{a}_2 \mathbf{a}_3^H \mathbf{a}_3) \cdot \mathbf{I} - (\mathbf{a}_3^H \mathbf{a}_2 \mathbf{a}_2^H \mathbf{a}_3) \cdot \mathbf{I} - (\mathbf{a}_3^H \mathbf{a}_3) \cdot \mathbf{a}_2 \mathbf{a}_2^H \right] \\ - (\mathbf{a}_2^H \mathbf{a}_2) \cdot \mathbf{a}_3 \mathbf{a}_3^H + (\mathbf{a}_3^H \mathbf{a}_2) \cdot \mathbf{a}_3 \mathbf{a}_2^H + (\mathbf{a}_2^H \mathbf{a}_3) \cdot \mathbf{a}_2 \mathbf{a}_3^H \end{array} \right\}}{\left[\sigma_n^4 + \sigma_{s2}^2 \sigma_n^2 \mathbf{a}_2^H \mathbf{a}_2 + \sigma_{s3}^2 \sigma_n^2 \mathbf{a}_3^H \mathbf{a}_3 + \sigma_{s2}^2 \sigma_{s3}^2 (\mathbf{a}_2^H \mathbf{a}_2 \mathbf{a}_3^H \mathbf{a}_3 - \mathbf{a}_3^H \mathbf{a}_2 \mathbf{a}_2^H \mathbf{a}_3) \right]}. \quad (37)$$

By letting $d_{ij} \equiv (1/p) \cdot \mathbf{a}_i^H \mathbf{a}_j$ for $i < j$ and using the fact that $\mathbf{a}_k^H \mathbf{a}_k = p$, $k = 1, 2, 3$, (37) can be rewritten as

$$\mathbf{Q}^{-1} = \frac{\sigma_n^{-2} \left\{ \begin{array}{l} \sigma_n^4 \mathbf{I} + \sigma_{s2}^2 \sigma_n^2 (p \mathbf{I} - \mathbf{a}_2 \mathbf{a}_2^H) + \sigma_{s3}^2 \sigma_n^2 (p \mathbf{I} - \mathbf{a}_3 \mathbf{a}_3^H) \\ + \sigma_{s2}^2 \sigma_{s3}^2 \left[p^2 (1 - |d_{23}|^2) \cdot \mathbf{I} - p \mathbf{a}_2 \mathbf{a}_2^H - p \mathbf{a}_3 \mathbf{a}_3^H \right] \\ + p d_{23}^* \mathbf{a}_3 \mathbf{a}_2^H + p d_{23} \mathbf{a}_2 \mathbf{a}_3^H \end{array} \right\}}{\sigma_n^4 + p \sigma_{s2}^2 \sigma_n^2 + p \sigma_{s3}^2 \sigma_n^2 + p^2 \sigma_{s2}^2 \sigma_{s3}^2 (1 - |d_{23}|^2)}. \quad (38)$$

Based on (38), we obtain the following expressions:

$$\mathbf{a}_1^H \mathbf{Q}^{-1} \mathbf{a}_1 = \frac{p \sigma_n^{-2} \left\{ \begin{array}{l} \sigma_n^4 + p \sigma_{s2}^2 \sigma_n^2 (1 - |d_{12}|^2) + p \sigma_{s3}^2 \sigma_n^2 (1 - |d_{13}|^2) \\ + p^2 \sigma_{s2}^2 \sigma_{s3}^2 [1 - |d_{23}|^2 - |d_{12}|^2 - |d_{13}|^2] \\ + 2 \operatorname{Re}(d_{12} d_{13}^* d_{23}) \end{array} \right\}}{\sigma_n^4 + p \sigma_{s2}^2 \sigma_n^2 + p \sigma_{s3}^2 \sigma_n^2 + p^2 \sigma_{s2}^2 \sigma_{s3}^2 (1 - |d_{23}|^2)}, \quad (39)$$

$$\mathbf{a}_1^H \mathbf{Q}^{-1} \mathbf{a}_2 = \frac{p \sigma_n^{-2} [\sigma_n^4 d_{12} + p \sigma_{s3}^2 \sigma_n^2 (d_{12} - d_{13} d_{23}^*)]}{\sigma_n^4 + p \sigma_{s2}^2 \sigma_n^2 + p \sigma_{s3}^2 \sigma_n^2 + p^2 \sigma_{s2}^2 \sigma_{s3}^2 (1 - |d_{23}|^2)}, \quad (40)$$

$$\mathbf{a}_1^H \mathbf{Q}^{-1} \mathbf{a}_3 = \frac{p \sigma_n^{-2} [\sigma_n^4 d_{13} + p \sigma_{s2}^2 \sigma_n^2 (d_{13} - d_{12} d_{23})]}{\sigma_n^4 + p \sigma_{s2}^2 \sigma_n^2 + p \sigma_{s3}^2 \sigma_n^2 + p^2 \sigma_{s2}^2 \sigma_{s3}^2 (1 - |d_{23}|^2)}, \quad (41)$$

$$\| \mathbf{Q}^{-1} \mathbf{a}_1 \|^2 = \frac{p\sigma_n^{-4} \left\{ \begin{aligned} & \sigma_n^8 + p\sigma_{s_2}^2\sigma_n^4 (p\sigma_{s_2}^2 + 2\sigma_n^2) (1 - |d_{12}|^2) + p\sigma_{s_3}^2\sigma_n^4 \\ & \times (p\sigma_{s_3}^2 + 2\sigma_n^2) (1 - |d_{13}|^2) + p^3\sigma_{s_2}^2\sigma_{s_3}^2 \\ & \times \left[2\sigma_{s_2}^2\sigma_n^2 + 2\sigma_{s_3}^2\sigma_n^2 + p\sigma_{s_2}^2\sigma_{s_3}^2 (1 - |d_{23}|^2) \right] \\ & \times \left[1 - |d_{23}|^2 - |d_{12}|^2 - |d_{13}|^2 + 2\text{Re}(d_{12}d_{13}^*d_{23}) \right] \\ & + 2p^2\sigma_{s_2}^2\sigma_{s_3}^2\sigma_n^4 \left[2 - |d_{23}|^2 - 2|d_{12}|^2 - 2|d_{13}|^2 \right. \\ & \left. + 3\text{Re}(d_{12}d_{13}^*d_{23}) \right] \end{aligned} \right\}}{\left[\sigma_n^4 + p\sigma_{s_2}^2\sigma_n^2 + p\sigma_{s_3}^2\sigma_n^2 + p^2\sigma_{s_2}^2\sigma_{s_3}^2 (1 - |d_{23}|^2) \right]^2}, \tag{42}$$

where $\text{Re}\{x\}$ and $\{x\}^*$ denote the real part and complex conjugation of x , respectively. Under adequate angular separation for each pair of the incident signal sources and appropriate inter-element spacing, we can assume that $|d_{ij}|^2 \ll 1$ for $i \neq j$ [2, 8]. Using this assumption and substituting (39)–(42) into P_{io} and P_{no} of (32) yields

$$\begin{aligned} P_{io} &\approx \frac{\sigma_{s_2}^2\sigma_n^4 |\sigma_n^2 d_{12} + p\sigma_{s_3}^2 d_{12}|^2 + \sigma_{s_3}^2\sigma_n^4 |\sigma_n^2 d_{13} + p\sigma_{s_2}^2 d_{13}|^2}{(\sigma_n^2 + p\sigma_{s_2}^2)^2 (\sigma_n^2 + p\sigma_{s_3}^2)^2} \\ &= \frac{\sigma_{s_2}^2\sigma_n^4 |d_{12}|^2}{(\sigma_n^2 + p\sigma_{s_2}^2)^2} + \frac{\sigma_{s_3}^2\sigma_n^4 |d_{13}|^2}{(\sigma_n^2 + p\sigma_{s_3}^2)^2} \end{aligned} \tag{43}$$

and

$$\begin{aligned} P_{no} &\approx \frac{\sigma_n^2 \left(\sigma_n^8 + p^2\sigma_{s_2}^4\sigma_n^4 + p^2\sigma_{s_3}^4\sigma_n^4 + 2p\sigma_{s_2}^2\sigma_n^6 + 2p\sigma_{s_3}^2\sigma_n^6 \right. \\ & \left. + 4p^2\sigma_{s_2}^2\sigma_{s_3}^2\sigma_n^4 + p^4\sigma_{s_2}^4\sigma_{s_3}^4 + 2p^3\sigma_{s_2}^4\sigma_{s_3}^2\sigma_n^2 + 2p^3\sigma_{s_2}^2\sigma_{s_3}^4\sigma_n^2 \right)}{p (\sigma_n^2 + p\sigma_{s_2}^2)^2 (\sigma_n^2 + p\sigma_{s_3}^2)^2} \\ &= \frac{\sigma_n^2}{p}, \end{aligned} \tag{44}$$

respectively. Hence, the approximated expression of $SINR_L$ for $q = 3$ is given by

$$SINR_L \approx \frac{\sigma_{s_1}^2}{\sum_{k=2}^3 \frac{\sigma_{s_k}^2\sigma_n^4 |d_{1k}|^2}{(\sigma_n^2 + p\sigma_{s_k}^2)^2} + \frac{\sigma_n^2}{p} + \frac{(p-1)\sigma_{s_1}^2}{m}}. \tag{45}$$

As compared with the results given by (14) and (32), the output SINR shown by (45) is expressed directly in terms of the system parameters. The $SINR_L$ for $q = 2$ and 1 can be obtained easily by substituting

$\sigma_{s3}^2 = 0$ and $\sigma_{s3}^2 = \sigma_{s2}^2 = 0$ into (45), respectively, as follows:

$$SINR_L|_{q=2} \approx \frac{\sigma_{s1}^2}{\frac{\sigma_{s2}^2 \sigma_n^4 |d_{12}|^2}{(\sigma_n^2 + p\sigma_{s2}^2)^2} + \frac{\sigma_n^2}{p} + \frac{(p-1)\sigma_{s1}^2}{m}}, \quad (46)$$

$$SINR_L|_{q=1} \approx \frac{\sigma_{s1}^2}{\frac{\sigma_n^2}{p} + \frac{(p-1)\sigma_{s1}^2}{m}}. \quad (47)$$

To obtain an explicit output SINR formula for any $3 < q < p$, a value of q should be specified in the \mathbf{Q}^{-1} of (36). Then, we substitute the \mathbf{Q}^{-1} into (32) and perform the required simplifications. However, it is not an easy task to derive the case for $q > 3$ due to the complicated algebraic manipulations. Instead, it is shown in Appendix A with mathematical induction [18, 19] that an approximation of $SINR_L$ for any $2 \leq q < p$ is given by

$$SINR_L \approx \frac{\sigma_{s1}^2}{P_{io} + P_{no} + P_c} \approx \frac{\sigma_{s1}^2}{\sum_{k=2}^q \frac{\sigma_{sk}^2 \sigma_n^4 |d_{1k}|^2}{(\sigma_n^2 + p\sigma_{sk}^2)^2} + \frac{\sigma_n^2}{p} + \frac{(p-1)\sigma_{s1}^2}{m}}. \quad (48)$$

Note that the condition of $q < p$ is required to satisfy $|d_{ij}|^2 \ll 1$ for $i \neq j$ in order to derive (45). For convenience, the derived formulas and corresponding assumptions are summarized in Table 1.

4. PERFORMANCE OF A LCMV BEAMFORMER WITH SIGNAL BLOCKING

4.1. Output SINR in Terms of \mathbf{Q}_B

Following the approximation $\hat{\mathbf{Q}} \approx \mathbf{Q}$ in $\hat{\mathbf{w}}$, $\hat{\mathbf{Q}}_B$ in (13) can be approximated by

$$\hat{\mathbf{Q}}_B = \mathbf{B}\hat{\mathbf{Q}}\mathbf{B}^H \approx \mathbf{B}\mathbf{Q}\mathbf{B}^H \equiv \mathbf{Q}_B. \quad (49)$$

Hence, we have

$$\hat{\mathbf{w}}_B \approx \frac{\mathbf{Q}_B^{-1}\mathbf{a}_1}{\mathbf{a}_1^H \mathbf{Q}_B^{-1} \mathbf{a}_1} \equiv \mathbf{w}_B. \quad (50)$$

Comparing (50) and (19), we note that the signal blocking replaces \mathbf{w}_o with \mathbf{w}_B and eliminates $\hat{\mathbf{w}}_c$. Since $\hat{\mathbf{w}}_c$ is the term caused by finite samples, the analysis of $\hat{\mathbf{w}}_B$ reduces to the infinite sample scenario under the same condition $m > 3p$ and approximation $\hat{\mathbf{Q}} \approx \mathbf{Q}$

considered in Section 3. This reveals that the condition $m > 3p$ is sufficient for a LCMV beamformer with signal blocking achieving to its infinite performance. To confirm this, a trial for the output SINRs computed by (11), (13), and (50) are plotted in Figure 3, where the four parameter settings are the same as those in Figure 2. The blocking matrices are produced by the “null” function in MATLAB to satisfy (10). We see from Figure 3 that most errors caused by the approximation used in (50) are within 1 dB or even less. This confirms that the exact performance of $\hat{\mathbf{w}}_B$ is insensitive to the data sample size m as compared with that of $\hat{\mathbf{w}}$.

Similar to (17), the output SINR of a LCMV beamformer with signal blocking is given by

$$SINR_B = \frac{\sigma_{s1}^2}{P_{i,B} + P_{n,B}} = \frac{\sigma_{s1}^2}{E \left[\sum_{k=2}^q \sigma_{sk}^2 |\hat{\mathbf{w}}_B^H \bar{\mathbf{a}}_k|^2 \right] + E [\sigma_n^2 \hat{\mathbf{w}}_B^H \hat{\mathbf{w}}_B]} \quad (51)$$

Table 1. The summary of the derived output SINR formulas.

	$SINR_L$	$SINR_B$	Assumptions
SINR in terms of \mathbf{Q} or \mathbf{Q}_B	(32)	(54)	1. $2 \leq q < p$ for $SINR_L$, $2 \leq q < N$ for $SINR_B$ 2. $\hat{\mathbf{w}} \approx \mathbf{w}_o + \hat{\mathbf{w}}_c$ and $\hat{\mathbf{w}}_B \approx \mathbf{w}_B$ are valid 3. \mathbf{B} satisfies (10)
Explicit SINR for $q = 3$	(45)	(68)	1. $q = 3$ 2. $\hat{\mathbf{w}} \approx \mathbf{w}_o + \hat{\mathbf{w}}_c$ and $\hat{\mathbf{w}}_B \approx \mathbf{w}_B$ are valid 3. $ d_{ij} ^2 \ll 1, d_{ij,B} ^2 \ll 1$ 4. \mathbf{B} satisfies (10) and (59)
Explicit SINR for general q	(48)	(69)	1. $2 \leq q < p$ for $SINR_L$, $2 \leq q < N$ for $SINR_B$ 2. $\hat{\mathbf{w}} \approx \mathbf{w}_o + \hat{\mathbf{w}}_c$ and $\hat{\mathbf{w}}_B \approx \mathbf{w}_B$ are valid 3. $ d_{ij} ^2 \ll 1, d_{ij,B} ^2 \ll 1$ 4. \mathbf{B} satisfies (10) and (59)
Explicit SINR for the Duvall beamformer	N/A	(80)	1. $2 \leq q < N$ 2. $\hat{\mathbf{w}}_B \approx \mathbf{w}_B$ is valid 3. $ d_{ij} ^2 \ll 1, d_{ij,B} ^2 \ll 1$ 4. Duvall’s \mathbf{B}

with

$$\begin{aligned}
 P_{i,B} &= E \left[\sum_{k=2}^q \sigma_{sk}^2 \left| \hat{\mathbf{w}}_B^H \bar{\mathbf{a}}_k \right|^2 \right] \\
 &\approx E \left[\sum_{k=2}^q \sigma_{sk}^2 \left| \mathbf{w}_B^H \bar{\mathbf{a}}_k \right|^2 \right] = \sum_{k=2}^q \sigma_{sk}^2 \left| \mathbf{w}_B^H \bar{\mathbf{a}}_k \right|^2 = \sum_{k=2}^q \sigma_{sk}^2 \left| \frac{\bar{\mathbf{a}}_1^H \mathbf{Q}_B^{-1} \bar{\mathbf{a}}_k}{\bar{\mathbf{a}}_1^H \mathbf{Q}_B^{-1} \bar{\mathbf{a}}_1} \right|^2 \quad (52)
 \end{aligned}$$

and

$$P_{n,B} = E \left[\sigma_n^2 \hat{\mathbf{w}}_B^H \hat{\mathbf{w}}_B \right] \approx \sigma_n^2 E \left[\mathbf{w}_B^H \mathbf{w}_B \right] = \sigma_n^2 \|\mathbf{w}_B\|^2 = \sigma_n^2 \frac{\|\mathbf{Q}_B^{-1} \bar{\mathbf{a}}_1\|^2}{(\bar{\mathbf{a}}_1^H \mathbf{Q}_B^{-1} \bar{\mathbf{a}}_1)^2}. \quad (53)$$

Substituting (52) and (53) into (51) yields

$$\text{SINR}_B = \frac{\sigma_{s1}^2}{P_{i,B} + P_{n,B}} \approx \frac{\sigma_{s1}^2}{\sum_{k=2}^q \sigma_{sk}^2 \left| \frac{\bar{\mathbf{a}}_1^H \mathbf{Q}_B^{-1} \bar{\mathbf{a}}_k}{\bar{\mathbf{a}}_1^H \mathbf{Q}_B^{-1} \bar{\mathbf{a}}_1} \right|^2 + \sigma_n^2 \frac{\|\mathbf{Q}_B^{-1} \bar{\mathbf{a}}_1\|^2}{(\bar{\mathbf{a}}_1^H \mathbf{Q}_B^{-1} \bar{\mathbf{a}}_1)^2}}. \quad (54)$$

Comparing (32) and (54), we observe that the cross power P_c produced by the cross weight $\hat{\mathbf{w}}_c$ is eliminated and the output power P_{i_o} and P_{n_o} produced by the optimal weight \mathbf{w}_o are replaced with $P_{i,B}$ and $P_{n,B}$, respectively when using signal blocking. If the sample size m is small or the desired signal power σ_{s1}^2 is large, the cross power P_c in the denominator of SINR_L will dominate and affect the

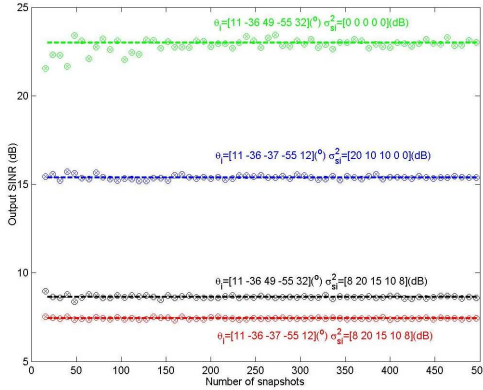


Figure 3. Output SINRs computed by three weight vectors. ‘o’: the weight vector in (11). ‘x’: the weight vector in (13). ‘- -’: the approximated weight vector in (50).

performance of a LCMV beamformer. On the contrary, no cross power is present in $SINR_B$. Hence, a LCMV beamformer with \mathbf{B} alleviates the finite sample effect on its performance. This leads to the fact that a LCMV beamformer with \mathbf{B} converges faster than the same beamformer without \mathbf{B} especially for large arrays or strong desired signal environments.

4.2. Derivation of \mathbf{Q}_B^{-1}

Analogous to the derivation of \mathbf{Q}^{-1} , we derive an expression for \mathbf{Q}_B^{-1} as follows. Let a set of dummy variables \mathbf{L}_r , $r = 1, 2, \dots, q$, be given by

$$\mathbf{L}_r = \begin{cases} \sigma_n^2 \mathbf{B}\mathbf{B}^H & r = 1 \\ \sum_{i=2}^r \sigma_{si}^2 \mathbf{B}\mathbf{a}_i \mathbf{a}_i^H \mathbf{B}^H + \sigma_n^2 \mathbf{B}\mathbf{B}^H & 2 \leq r \leq q \end{cases} \quad (55)$$

\mathbf{Q}_B^{-1} can be expressed by

$$\mathbf{Q}_B^{-1} = \mathbf{L}_q^{-1} = (\mathbf{L}_{q-1} + \sigma_{sq}^2 \mathbf{B}\mathbf{a}_q \mathbf{a}_q^H \mathbf{B}^H)^{-1} \quad (56)$$

Using the matrix inversion lemma, we have \mathbf{Q}_B^{-1} given by

$$\mathbf{Q}_B^{-1} = \mathbf{L}_q^{-1} = \mathbf{L}_{q-1}^{-1} \left(\mathbf{I} - \frac{\mathbf{B}\mathbf{a}_q \mathbf{a}_q^H \mathbf{B}^H \mathbf{L}_{q-1}^{-1}}{\sigma_{sq}^{-2} + \mathbf{a}_q^H \mathbf{B}^H \mathbf{L}_{q-1}^{-1} \mathbf{B}\mathbf{a}_q} \right) \quad (57)$$

with $\mathbf{L}_1^{-1} = \sigma_n^{-2} (\mathbf{B}\mathbf{B}^H)^{-1}$. It follows from (57) that

$$\begin{aligned} \mathbf{Q}_B^{-1} &= \underbrace{\sigma_n^{-2} (\mathbf{B}\mathbf{B}^H)^{-1}}_{\mathbf{L}_1^{-1}} \underbrace{\left(\mathbf{I} - \frac{\mathbf{B}\mathbf{a}_2 \mathbf{a}_2^H \mathbf{B}^H \mathbf{L}_1^{-1}}{\sigma_{s2}^{-2} + \mathbf{a}_2^H \mathbf{B}^H \mathbf{L}_1^{-1} \mathbf{B}\mathbf{a}_2} \right)}_{\mathbf{L}_2^{-1}} \underbrace{\left(\mathbf{I} - \frac{\mathbf{B}\mathbf{a}_3 \mathbf{a}_3^H \mathbf{B}^H \mathbf{L}_2^{-1}}{\sigma_{s3}^{-2} + \mathbf{a}_3^H \mathbf{B}^H \mathbf{L}_2^{-1} \mathbf{B}\mathbf{a}_3} \right)}_{\mathbf{L}_3^{-1}} \\ &\quad \dots \left(\mathbf{I} - \frac{\mathbf{B}\mathbf{a}_q \mathbf{a}_q^H \mathbf{B}^H \mathbf{L}_{q-1}^{-1}}{\sigma_{sq}^{-2} + \mathbf{a}_q^H \mathbf{B}^H \mathbf{L}_{q-1}^{-1} \mathbf{B}\mathbf{a}_q} \right) \\ &= \sigma_n^{-2} (\mathbf{B}\mathbf{B}^H)^{-1} \prod_{i=2}^q \left(\mathbf{I} - \frac{\mathbf{B}\mathbf{a}_i \mathbf{a}_i^H \mathbf{B}^H \mathbf{L}_{i-1}^{-1}}{\sigma_{si}^{-2} + \mathbf{a}_i^H \mathbf{B}^H \mathbf{L}_{i-1}^{-1} \mathbf{B}\mathbf{a}_i} \right). \end{aligned} \quad (58)$$

Substituting (58) into (54) yields an explicit formula for computing $SINR_B$ under any q interferers.

4.3. Output SINR for Two Interferers

In direct form beamformers, the blocking matrix usually possesses the property [5, 8]

$$\mathbf{B}\mathbf{a}_k = \gamma_k \bar{\mathbf{a}}_k, \quad k = 2, \dots, q \quad (59)$$

in addition to (10), where the scalar γ_k depends on the category of \mathbf{B} . The constraint of (59) preserves the directions of all interferers, so that $\hat{\mathbf{w}}_B$ can put the nulls in the direction angles $\theta_2, \dots, \theta_q$ [5]. A systematic methodology to design the blocking matrices satisfying both (10) and (59) is presented in [8], which is appropriate for a ULA. Here, we consider the blocking matrices in [8] and derive $SINR_B$ under two interferers, i.e., $q = 3$.

The steering vector \mathbf{a}_k of a ULA is given by

$$\begin{aligned} \mathbf{a}_k &= [1 \quad \exp(i\varphi_k) \quad \exp(i2\varphi_k) \quad \dots \quad \exp(i(p-1)\varphi_k)]^T \\ &= [1 \quad z_k \quad z_k^2 \quad \dots \quad z_k^{p-1}]^T, \end{aligned} \tag{60}$$

where $z_k = \exp(i\varphi_k)$, $\varphi_k = 2\pi(d/\lambda)\sin\theta_k$. d is the inter-element spacing, λ the signal wavelength, and θ_k the direction angle off broadside for the k th signal source, $k = 1, 2, \dots, q$. The superscript “ T ” denotes the transpose operation. Setting $q = 3$ in (58), performing some algebraic manipulations, and utilizing the relationship of (59), we obtain

$$\mathbf{Q}_B^{-1} = \frac{\sigma_n^{-2} \left\{ \begin{aligned} &\sigma_n^4 (\mathbf{B}\mathbf{B}^H)^{-1} + |\gamma_2|^2 \sigma_{s_2}^2 \sigma_n^2 \left[\overline{\mathbf{a}}_2^H (\mathbf{B}\mathbf{B}^H)^{-1} \overline{\mathbf{a}}_2 \right] \\ &\cdot (\mathbf{B}\mathbf{B}^H)^{-1} - (\mathbf{B}\mathbf{B}^H)^{-1} \overline{\mathbf{a}}_2 \overline{\mathbf{a}}_2^H (\mathbf{B}\mathbf{B}^H)^{-1} \\ &+ |\gamma_2|^2 \sigma_{s_2}^2 |\gamma_3|^2 \sigma_{s_3}^2 \\ &\left[\overline{\mathbf{a}}_2^H (\mathbf{B}\mathbf{B}^H)^{-1} \overline{\mathbf{a}}_2 \overline{\mathbf{a}}_3^H (\mathbf{B}\mathbf{B}^H)^{-1} \overline{\mathbf{a}}_3 \right] \cdot (\mathbf{B}\mathbf{B}^H)^{-1} \\ &- \left(\overline{\mathbf{a}}_3^H (\mathbf{B}\mathbf{B}^H)^{-1} \overline{\mathbf{a}}_2 \overline{\mathbf{a}}_2^H (\mathbf{B}\mathbf{B}^H)^{-1} \overline{\mathbf{a}}_3 \right) \cdot (\mathbf{B}\mathbf{B}^H)^{-1} \\ &- \left(\overline{\mathbf{a}}_2^H (\mathbf{B}\mathbf{B}^H)^{-1} \overline{\mathbf{a}}_2 \right) \cdot (\mathbf{B}\mathbf{B}^H)^{-1} \overline{\mathbf{a}}_3 \overline{\mathbf{a}}_3^H (\mathbf{B}\mathbf{B}^H)^{-1} \\ &- \left(\overline{\mathbf{a}}_3^H (\mathbf{B}\mathbf{B}^H)^{-1} \overline{\mathbf{a}}_3 \right) \cdot (\mathbf{B}\mathbf{B}^H)^{-1} \overline{\mathbf{a}}_2 \overline{\mathbf{a}}_2^H (\mathbf{B}\mathbf{B}^H)^{-1} \\ &+ \left(\overline{\mathbf{a}}_2^H (\mathbf{B}\mathbf{B}^H)^{-1} \overline{\mathbf{a}}_3 \right) \cdot (\mathbf{B}\mathbf{B}^H)^{-1} \overline{\mathbf{a}}_2 \overline{\mathbf{a}}_3^H (\mathbf{B}\mathbf{B}^H)^{-1} \\ &+ \left(\overline{\mathbf{a}}_3^H (\mathbf{B}\mathbf{B}^H)^{-1} \overline{\mathbf{a}}_2 \right) \cdot (\mathbf{B}\mathbf{B}^H)^{-1} \overline{\mathbf{a}}_3 \overline{\mathbf{a}}_2^H (\mathbf{B}\mathbf{B}^H)^{-1} \\ &+ |\gamma_3|^2 \sigma_{s_3}^2 \sigma_n^2 \left[\overline{\mathbf{a}}_3^H (\mathbf{B}\mathbf{B}^H)^{-1} \overline{\mathbf{a}}_3 \right] \cdot (\mathbf{B}\mathbf{B}^H)^{-1} \\ &- (\mathbf{B}\mathbf{B}^H)^{-1} \overline{\mathbf{a}}_3 \overline{\mathbf{a}}_3^H (\mathbf{B}\mathbf{B}^H)^{-1} \end{aligned} \right\}}{\begin{aligned} &\sigma_n^4 + |\gamma_2|^2 \sigma_{s_2}^2 \sigma_n^2 \overline{\mathbf{a}}_2^H (\mathbf{B}\mathbf{B}^H)^{-1} \overline{\mathbf{a}}_2 + |\gamma_3|^2 \sigma_{s_3}^2 \sigma_n^2 \overline{\mathbf{a}}_3^H (\mathbf{B}\mathbf{B}^H)^{-1} \overline{\mathbf{a}}_3 \\ &+ |\gamma_2|^2 \sigma_{s_2}^2 |\gamma_3|^2 \sigma_{s_3}^2 \left(\overline{\mathbf{a}}_2^H (\mathbf{B}\mathbf{B}^H)^{-1} \overline{\mathbf{a}}_2 \overline{\mathbf{a}}_3^H (\mathbf{B}\mathbf{B}^H)^{-1} \overline{\mathbf{a}}_3 \right) \\ &\left[-\overline{\mathbf{a}}_3^H (\mathbf{B}\mathbf{B}^H)^{-1} \overline{\mathbf{a}}_2 \overline{\mathbf{a}}_2^H (\mathbf{B}\mathbf{B}^H)^{-1} \overline{\mathbf{a}}_3 \right] \end{aligned}} \tag{61}$$

Let $d_{ij,B} = \overline{\mathbf{a}}_i^H (\mathbf{B}\mathbf{B}^H)^{-1} \overline{\mathbf{a}}_j / (\sqrt{\overline{\mathbf{a}}_i^H (\mathbf{B}\mathbf{B}^H)^{-1} \overline{\mathbf{a}}_i} \sqrt{\overline{\mathbf{a}}_j^H (\mathbf{B}\mathbf{B}^H)^{-1} \overline{\mathbf{a}}_j})$, $i <$

j. Based on (61), it is straightforward to derive the following terms:

$$\mathbf{a}_1^H \mathbf{Q}_B^{-1} \mathbf{a}_1 = \frac{\sigma_n^{-2} \left\{ \begin{aligned} &\sigma_n^4 \overline{\mathbf{a}_1}^H (\mathbf{B}\mathbf{B}^H)^{-1} \overline{\mathbf{a}_1} + |\gamma_2|^2 \sigma_{s_2}^2 \sigma_n^2 \overline{\mathbf{a}_1}^H (\mathbf{B}\mathbf{B}^H)^{-1} \overline{\mathbf{a}_1} \\ &\overline{\mathbf{a}_2}^H (\mathbf{B}\mathbf{B}^H)^{-1} \overline{\mathbf{a}_2} (1 - |d_{12,B}|^2) + |\gamma_3|^2 \sigma_{s_3}^2 \sigma_n^2 \overline{\mathbf{a}_1}^H (\mathbf{B}\mathbf{B}^H)^{-1} \\ &\overline{\mathbf{a}_3} (1 - |d_{13,B}|^2) + |\gamma_2|^2 \sigma_{s_2}^2 |\gamma_3|^2 \sigma_{s_3}^2 \overline{\mathbf{a}_1}^H \\ &(\mathbf{B}\mathbf{B}^H)^{-1} \overline{\mathbf{a}_1} \overline{\mathbf{a}_2}^H (\mathbf{B}\mathbf{B}^H)^{-1} \overline{\mathbf{a}_2} \overline{\mathbf{a}_3}^H (\mathbf{B}\mathbf{B}^H)^{-1} \overline{\mathbf{a}_3} \\ &\times [1 - |d_{23,B}|^2 - |d_{12,B}|^2 - |d_{13,B}|^2 + 2\text{Re}(d_{12,B} d_{13,B}^* d_{23,B})] \end{aligned} \right\}}{\left[\begin{aligned} &\sigma_n^4 + |\gamma_2|^2 \sigma_{s_2}^2 \sigma_n^2 \overline{\mathbf{a}_2}^H (\mathbf{B}\mathbf{B}^H)^{-1} \overline{\mathbf{a}_2} + |\gamma_3|^2 \sigma_{s_3}^2 \sigma_n^2 \overline{\mathbf{a}_3}^H (\mathbf{B}\mathbf{B}^H)^{-1} \overline{\mathbf{a}_3} \\ &+ |\gamma_2|^2 \sigma_{s_2}^2 |\gamma_3|^2 \sigma_{s_3}^2 \overline{\mathbf{a}_2}^H (\mathbf{B}\mathbf{B}^H)^{-1} \overline{\mathbf{a}_2} \overline{\mathbf{a}_3}^H (\mathbf{B}\mathbf{B}^H)^{-1} \overline{\mathbf{a}_3} (1 - |d_{23,B}|^2) \end{aligned} \right]}, \quad (62)$$

$$\mathbf{a}_1^H \mathbf{Q}_B^{-1} \mathbf{a}_2 = \frac{\sigma_n^{-2} \left[\begin{aligned} &\sigma_n^4 \sqrt{\overline{\mathbf{a}_1}^H (\mathbf{B}\mathbf{B}^H)^{-1} \overline{\mathbf{a}_1}} \sqrt{\overline{\mathbf{a}_2}^H (\mathbf{B}\mathbf{B}^H)^{-1} \overline{\mathbf{a}_2}} d_{12,B} + |\gamma_3|^2 \sigma_{s_3}^2 \\ &\sigma_n^2 \overline{\mathbf{a}_3}^H (\mathbf{B}\mathbf{B}^H)^{-1} \overline{\mathbf{a}_3} \sqrt{\overline{\mathbf{a}_1}^H (\mathbf{B}\mathbf{B}^H)^{-1} \overline{\mathbf{a}_1}} \sqrt{\overline{\mathbf{a}_2}^H (\mathbf{B}\mathbf{B}^H)^{-1} \overline{\mathbf{a}_2}} \\ &(d_{12,B} - d_{13,B} d_{23,B}^*) \end{aligned} \right]}{\left[\begin{aligned} &\sigma_n^4 + |\gamma_2|^2 \sigma_{s_2}^2 \sigma_n^2 \overline{\mathbf{a}_2}^H (\mathbf{B}\mathbf{B}^H)^{-1} \overline{\mathbf{a}_2} + |\gamma_3|^2 \sigma_{s_3}^2 \sigma_n^2 \overline{\mathbf{a}_3}^H (\mathbf{B}\mathbf{B}^H)^{-1} \\ &\overline{\mathbf{a}_3} + |\gamma_2|^2 \sigma_{s_2}^2 |\gamma_3|^2 \sigma_{s_3}^2 \overline{\mathbf{a}_2}^H (\mathbf{B}\mathbf{B}^H)^{-1} \overline{\mathbf{a}_2} \overline{\mathbf{a}_3}^H (\mathbf{B}\mathbf{B}^H)^{-1} \overline{\mathbf{a}_3} (1 - |d_{23,B}|^2) \end{aligned} \right]}, \quad (63)$$

$$\mathbf{a}_1^H \mathbf{Q}_B^{-1} \mathbf{a}_3 = \frac{\sigma_n^{-2} \left[\begin{aligned} &\sigma_n^4 \sqrt{\overline{\mathbf{a}_1}^H (\mathbf{B}\mathbf{B}^H)^{-1} \overline{\mathbf{a}_1}} \sqrt{\overline{\mathbf{a}_3}^H (\mathbf{B}\mathbf{B}^H)^{-1} \overline{\mathbf{a}_3}} d_{13,B} + |\gamma_2|^2 \\ &\sigma_{s_2}^2 \sigma_n^2 \overline{\mathbf{a}_2}^H (\mathbf{B}\mathbf{B}^H)^{-1} \overline{\mathbf{a}_2} \times \sqrt{\overline{\mathbf{a}_1}^H (\mathbf{B}\mathbf{B}^H)^{-1} \overline{\mathbf{a}_1}} \\ &\sqrt{\overline{\mathbf{a}_3}^H (\mathbf{B}\mathbf{B}^H)^{-1} \overline{\mathbf{a}_3}} (d_{13,B} - d_{12,B} d_{23,B}) \end{aligned} \right]}{\left[\begin{aligned} &\sigma_n^4 + |\gamma_2|^2 \sigma_{s_2}^2 \sigma_n^2 \overline{\mathbf{a}_2}^H (\mathbf{B}\mathbf{B}^H)^{-1} \overline{\mathbf{a}_2} + |\gamma_3|^2 \sigma_{s_3}^2 \sigma_n^2 \overline{\mathbf{a}_3}^H \\ &(\mathbf{B}\mathbf{B}^H)^{-1} \overline{\mathbf{a}_3} + |\gamma_2|^2 \sigma_{s_2}^2 |\gamma_3|^2 \sigma_{s_3}^2 \overline{\mathbf{a}_2}^H (\mathbf{B}\mathbf{B}^H)^{-1} \overline{\mathbf{a}_2} \\ &\overline{\mathbf{a}_3}^H (\mathbf{B}\mathbf{B}^H)^{-1} \overline{\mathbf{a}_3} (1 - |d_{23,B}|^2) \end{aligned} \right]}, \quad (64)$$

$$\|\mathbf{Q}_B^{-1} \mathbf{a}_1\|^2 = \frac{\sigma_n^{-4} \left\| \begin{aligned} &\sigma_n^4 (\mathbf{B}\mathbf{B}^H)^{-1} \overline{\mathbf{a}_1} + |\gamma_2|^2 \sigma_{s_2}^2 \sigma_n^2 \left[(\overline{\mathbf{a}_2}^H (\mathbf{B}\mathbf{B}^H)^{-1} \overline{\mathbf{a}_2}) (\mathbf{B}\mathbf{B}^H)^{-1} \overline{\mathbf{a}_1} \right]^2 \\ &- (\overline{\mathbf{a}_2}^H (\mathbf{B}\mathbf{B}^H)^{-1} \overline{\mathbf{a}_1}) \cdot (\mathbf{B}\mathbf{B}^H)^{-1} \overline{\mathbf{a}_2} + |\gamma_2|^2 \sigma_{s_2}^2 |\gamma_3|^2 \sigma_{s_3}^2 \\ &\left[\overline{\mathbf{a}_2}^H (\mathbf{B}\mathbf{B}^H)^{-1} \overline{\mathbf{a}_2} \overline{\mathbf{a}_3}^H (\mathbf{B}\mathbf{B}^H)^{-1} \overline{\mathbf{a}_3} (1 - |d_{23,B}|^2) (\mathbf{B}\mathbf{B}^H)^{-1} \overline{\mathbf{a}_1} \right] \\ &- \overline{\mathbf{a}_3}^H (\mathbf{B}\mathbf{B}^H)^{-1} \overline{\mathbf{a}_3} \sqrt{\overline{\mathbf{a}_2}^H (\mathbf{B}\mathbf{B}^H)^{-1} \overline{\mathbf{a}_2}} \sqrt{\overline{\mathbf{a}_1}^H (\mathbf{B}\mathbf{B}^H)^{-1} \overline{\mathbf{a}_1}} \\ &(d_{12,B}^* - d_{23,B} d_{13,B}^*) (\mathbf{B}\mathbf{B}^H)^{-1} \overline{\mathbf{a}_2} - \overline{\mathbf{a}_2}^H (\mathbf{B}\mathbf{B}^H)^{-1} \overline{\mathbf{a}_2} \\ &\sqrt{\overline{\mathbf{a}_1}^H (\mathbf{B}\mathbf{B}^H)^{-1} \overline{\mathbf{a}_1}} \times \sqrt{\overline{\mathbf{a}_3}^H (\mathbf{B}\mathbf{B}^H)^{-1} \overline{\mathbf{a}_3}} \\ &(d_{13,B}^* - d_{12,B}^* d_{23,B}^*) \cdot (\mathbf{B}\mathbf{B}^H)^{-1} \overline{\mathbf{a}_3} \\ &+ |\gamma_3|^2 \sigma_{s_3}^2 \sigma_n^2 \left[(\overline{\mathbf{a}_3}^H (\mathbf{B}\mathbf{B}^H)^{-1} \overline{\mathbf{a}_3}) \cdot (\mathbf{B}\mathbf{B}^H)^{-1} \overline{\mathbf{a}_1} \right] \\ &- (\overline{\mathbf{a}_3}^H (\mathbf{B}\mathbf{B}^H)^{-1} \overline{\mathbf{a}_1}) \cdot (\mathbf{B}\mathbf{B}^H)^{-1} \overline{\mathbf{a}_3} \end{aligned} \right\|}{\left[\begin{aligned} &\sigma_n^4 + |\gamma_2|^2 \sigma_{s_2}^2 \sigma_n^2 \overline{\mathbf{a}_2}^H (\mathbf{B}\mathbf{B}^H)^{-1} \overline{\mathbf{a}_2} + |\gamma_3|^2 \sigma_{s_3}^2 \sigma_n^2 \overline{\mathbf{a}_3}^H \\ &(\mathbf{B}\mathbf{B}^H)^{-1} \overline{\mathbf{a}_3} + |\gamma_2|^2 \sigma_{s_2}^2 |\gamma_3|^2 \sigma_{s_3}^2 \overline{\mathbf{a}_2}^H (\mathbf{B}\mathbf{B}^H)^{-1} \overline{\mathbf{a}_2} \overline{\mathbf{a}_3}^H \\ &(\mathbf{B}\mathbf{B}^H)^{-1} \overline{\mathbf{a}_3} (1 - |d_{23,B}|^2) \end{aligned} \right]}^2. \quad (65)$$

Substituting (62)–(65) into (54) under $q = 3$ and $|d_{ij,B}|^2 \ll 1$, $i \neq j$, we obtain

$$P_{i,B} \approx \sum_{k=2}^3 \frac{\sigma_{sk}^2 \sigma_n^4 \bar{\mathbf{a}}_k^H (\mathbf{B}\mathbf{B}^H)^{-1} \bar{\mathbf{a}}_k |d_{1k,B}|^2}{\bar{\mathbf{a}}_1^H (\mathbf{B}\mathbf{B}^H)^{-1} \bar{\mathbf{a}}_1 [\sigma_n^2 + |\gamma_k|^2 \sigma_{sk}^2 \bar{\mathbf{a}}_k^H (\mathbf{B}\mathbf{B}^H)^{-1} \bar{\mathbf{a}}_k]^2} \quad (66)$$

and

$$P_{n,B} \approx \sigma_n^2 \frac{\bar{\mathbf{a}}_1^H (\mathbf{B}\mathbf{B}^H)^{-1} (\mathbf{B}\mathbf{B}^H)^{-1} \bar{\mathbf{a}}_1}{[\bar{\mathbf{a}}_1^H (\mathbf{B}\mathbf{B}^H)^{-1} \bar{\mathbf{a}}_1]^2}. \quad (67)$$

Therefore, the output SINR of a LCMV beamformer with \mathbf{B} satisfying (10) and (59) is approximately given by

$$\begin{aligned} SINR_B \approx & \frac{\sigma_{s1}^2}{\sum_{k=2}^3 \frac{\sigma_{sk}^2 \sigma_n^4 \bar{\mathbf{a}}_k^H (\mathbf{B}\mathbf{B}^H)^{-1} \bar{\mathbf{a}}_k |d_{1k,B}|^2}{\bar{\mathbf{a}}_1^H (\mathbf{B}\mathbf{B}^H)^{-1} \bar{\mathbf{a}}_1 [\sigma_n^2 + |\gamma_k|^2 \sigma_{sk}^2 \bar{\mathbf{a}}_k^H (\mathbf{B}\mathbf{B}^H)^{-1} \bar{\mathbf{a}}_k]^2} + \sigma_n^2 \frac{\bar{\mathbf{a}}_1^H (\mathbf{B}\mathbf{B}^H)^{-1} (\mathbf{B}\mathbf{B}^H)^{-1} \bar{\mathbf{a}}_1}{[\bar{\mathbf{a}}_1^H (\mathbf{B}\mathbf{B}^H)^{-1} \bar{\mathbf{a}}_1]^2}}. \quad (68) \end{aligned}$$

Note that $P_{i,B}$ and $P_{n,B}$ of (68) reduce to P_{io} and P_{no} of (45) if \mathbf{B} , γ_k , $\bar{\mathbf{a}}_1$, and $\bar{\mathbf{a}}_k$ are replaced by \mathbf{I} , 1, \mathbf{a}_1 , and \mathbf{a}_k , respectively, which confirms the validity of (68). Similar to (45)–(48), it is shown in Appendix B that the $SINR_B$ in (68) can be generalized to the q -interferer case, $2 \leq q < N$, as follows:

$$\begin{aligned} SINR_B &= \frac{\sigma_{s1}^2}{P_{i,B} + P_{n,B}} \\ &\approx \frac{\sigma_{s1}^2}{\sum_{k=2}^q \frac{\sigma_{sk}^2 \sigma_n^4 \bar{\mathbf{a}}_k^H (\mathbf{B}\mathbf{B}^H)^{-1} \bar{\mathbf{a}}_k |d_{1k,B}|^2}{\bar{\mathbf{a}}_1^H (\mathbf{B}\mathbf{B}^H)^{-1} \bar{\mathbf{a}}_1 [\sigma_n^2 + |\gamma_k|^2 \sigma_{sk}^2 \bar{\mathbf{a}}_k^H (\mathbf{B}\mathbf{B}^H)^{-1} \bar{\mathbf{a}}_k]^2} + \sigma_n^2 \frac{\bar{\mathbf{a}}_1^H (\mathbf{B}\mathbf{B}^H)^{-1} (\mathbf{B}\mathbf{B}^H)^{-1} \bar{\mathbf{a}}_1}{[\bar{\mathbf{a}}_1^H (\mathbf{B}\mathbf{B}^H)^{-1} \bar{\mathbf{a}}_1]^2}}. \quad (69) \end{aligned}$$

The generalized result of (69) is reasonable when the approximation used in (50) and $|d_{ij,B}|^2 \ll 1$, $i \neq j$, hold. An example with common source directions and moderate sample size is presented in Section 5 to confirm the accuracy of (69) and the following formulas.

4.4. The Duvall Beamformer

To see the details about the effect of the signal blocking on P_{io} and P_{no} of (48), we consider the following \mathbf{B} used by the Duvall beamformer [4]:

$$\mathbf{B} = \begin{bmatrix} -z_1 & 1 & 0 & 0 & \cdots & 0 \\ 0 & -z_1 & 1 & 0 & \cdots & 0 \\ 0 & 0 & -z_1 & 1 & \ddots & \vdots \\ \vdots & \vdots & \ddots & \ddots & \ddots & \vdots \\ 0 & 0 & \cdots & 0 & -z_1 & 1 \end{bmatrix}_{(p-1) \times p} \quad (70)$$

and

$$\gamma_k = z_k - z_1 = \exp(i\varphi_k) - \exp(i\varphi_1). \quad (71)$$

Based on the blocking matrix of (70), we can further derive the terms $\bar{\mathbf{a}}_k^H (\mathbf{B}\mathbf{B}^H)^{-1} \bar{\mathbf{a}}_k$, $\bar{\mathbf{a}}_1^H (\mathbf{B}\mathbf{B}^H)^{-1} \bar{\mathbf{a}}_1$, and $\bar{\mathbf{a}}_1^H (\mathbf{B}\mathbf{B}^H)^{-1} (\mathbf{B}\mathbf{B}^H)^{-1} \bar{\mathbf{a}}_1$ in $P_{i,B}$ and $P_{n,B}$ of (69). Following the well-known Gauss-Jordan elimination algorithm [20] and performing some algebraic manipulations, we have the term $(\mathbf{B}\mathbf{B}^H)^{-1}$ given by

$$\begin{aligned} (\mathbf{B}\mathbf{B}^H)^{-1} &= \frac{1}{p} \begin{bmatrix} p-1 & p-2 & p-3 & \cdots & 1 \\ p-2 & 2(p-2) & 2(p-3) & \cdots & 2 \\ p-3 & 2(p-3) & 3(p-3) & \cdots & 3 \\ \vdots & \vdots & \vdots & \ddots & \vdots \\ 1 & 2 & 3 & \cdots & p-1 \end{bmatrix} \\ &\otimes \begin{bmatrix} 1 & z_1^* & (z_1^*)^2 & \cdots & (z_1^*)^{p-2} \\ z_1 & 1 & z_1^* & \cdots & (z_1^*)^{p-3} \\ z_1^2 & z_1 & 1 & \ddots & \vdots \\ \vdots & \vdots & \ddots & \ddots & z_1^* \\ z_1^{p-2} & z_1^{p-3} & \cdots & z_1 & 1 \end{bmatrix}, \end{aligned} \quad (72)$$

where “ \otimes ” denotes the Hadamard product. It follows from (72) and some necessary algebraic manipulations that

$$\begin{aligned} &\bar{\mathbf{a}}_k^H (\mathbf{B}\mathbf{B}^H)^{-1} \bar{\mathbf{a}}_k \\ &= \frac{p^2 - 1}{6} + \frac{1}{3p} \sum_{t=1}^{p-2} (p-t-1)(p-t)(p-t+1) \cos[t(\varphi_k - \varphi_1)]. \end{aligned} \quad (73)$$

We show in Appendix C that (73) can have a closed-form expression as follows:

$$\bar{\mathbf{a}}_k^H (\mathbf{B}\mathbf{B}^H)^{-1} \bar{\mathbf{a}}_k = \frac{p^2 [1 - \cos(\varphi_k - \varphi_1)] + \cos[p(\varphi_k - \varphi_1)] - 1}{2p [1 - \cos(\varphi_k - \varphi_1)]^2}. \quad (74)$$

Based on (74), we can substitute $k = 1$ and apply L' Hopital’s rule to obtain

$$\bar{\mathbf{a}}_1^H (\mathbf{B}\mathbf{B}^H)^{-1} \bar{\mathbf{a}}_1 = \frac{p(p^2 - 1)}{12}. \quad (75)$$

Moreover, since the square of the absolute value of d_{1k} can be simplified to

$$|d_{1k}|^2 = \frac{1 - \cos[p(\varphi_k - \varphi_1)]}{p^2 [1 - \cos(\varphi_k - \varphi_1)]} \quad (76)$$

according to (60), the condition $|d_{1k}|^2 \ll 1$ is equivalent to $1 - \cos[p(\varphi_k - \varphi_1)] \ll p^2 [1 - \cos(\varphi_k - \varphi_1)]$. Hence, we have the following approximations for $\bar{\mathbf{a}}_k^H (\mathbf{B}\mathbf{B}^H)^{-1} \bar{\mathbf{a}}_k$ of (74) and $|\gamma_k|^2 \bar{\mathbf{a}}_k^H (\mathbf{B}\mathbf{B}^H)^{-1} \bar{\mathbf{a}}_k$:

$$\begin{aligned} \bar{\mathbf{a}}_k^H (\mathbf{B}\mathbf{B}^H)^{-1} \bar{\mathbf{a}}_k &\approx \frac{p}{2 [1 - \cos(\varphi_k - \varphi_1)]} \\ \text{and } |\gamma_k|^2 \bar{\mathbf{a}}_k^H (\mathbf{B}\mathbf{B}^H)^{-1} \bar{\mathbf{a}}_k &\approx p. \end{aligned} \quad (77)$$

Next, we consider the term $\bar{\mathbf{a}}_1^H (\mathbf{B}\mathbf{B}^H)^{-1} (\mathbf{B}\mathbf{B}^H)^{-1} \bar{\mathbf{a}}_1$. Using (60) and (72), we have

$$\begin{aligned} &(\mathbf{B}\mathbf{B}^H)^{-1} \bar{\mathbf{a}}_1 \\ &= \left[\frac{p-1}{2} (p-2) z_1 \quad \frac{3}{2} (p-3) z_1^2 \quad \dots \quad \frac{3}{2} (p-3) z_1^{p-4} (p-2) z_1^{p-3} \frac{p-1}{2} z_1^{p-2} \right]^T. \end{aligned} \quad (78)$$

Note that the i th and $(p-i)$ th entries of (78) have the same coefficients. The closed-form of $\bar{\mathbf{a}}_1^H (\mathbf{B}\mathbf{B}^H)^{-1} (\mathbf{B}\mathbf{B}^H)^{-1} \bar{\mathbf{a}}_1$ can be obtained by taking the squared norm of (78) as follows:

$$\bar{\mathbf{a}}_1^H (\mathbf{B}\mathbf{B}^H)^{-1} (\mathbf{B}\mathbf{B}^H)^{-1} \bar{\mathbf{a}}_1 = \frac{p(p^4 - 1)}{120}. \quad (79)$$

Substituting (75), (77), and (79) into (69), we have an explicit expression for the output SINR of the Duvall beamformer as follows:

$$\begin{aligned} \text{SINR}_B &= \frac{\sigma_{s1}^2}{P_{i,B} + P_{n,B}} \\ &\approx \frac{\sigma_{s1}^2}{\sum_{k=2}^q \frac{6}{(p^2-1)[1-\cos(\varphi_k-\varphi_1)]} \cdot \frac{\sigma_{sk}^2 \sigma_n^4 |d_{1k,B}|^2}{(\sigma_n^2 + p\sigma_{sk}^2)^2} + \frac{\sigma_n^2}{p} \cdot \frac{6(p^2+1)}{5(p^2-1)}}. \end{aligned} \quad (80)$$

The summary of the derived SINR formulas in Sections 3–4 is presented in Table 1.

Unlike (14) and (15), the comparison of (48) and (80) provides insights into the influence on performance when the blocking matrix of (70) is used. From (48) and (80), it is apparent that $P_{n,B}$ is always larger than P_{no} . Comparing P_{io} and $P_{i,B}$, the main difference between them is the ratio $6/\{(p^2-1)[1-\cos(\varphi_k-\varphi_1)]\}$ in each summation term. $|d_{1k}|^2$ and $|d_{1k,B}|^2$ are assumed to be tiny and have almost the same scale. More details about $|d_{1k,B}|^2$ are presented in Appendix D. Since all sources are assumed to have distinct incident angles with enough

angular separations, $6/\{(p^2 - 1)[1 - \cos(\varphi_k - \varphi_1)]\}$ is normally smaller than one. Therefore, it is possible for $P_{i,B}$ to be smaller than P_{io} , but this improvement is slight due to the fact that P_{io} is relative marginal as compared with P_{no} [2]. Besides, it is reasonable that $P_{i,B} + P_{n,B}$ is always larger than $P_{io} + P_{no}$ owing to the loss of the degree of freedom (DOF). As a result, inserting the blocking matrix operation into LCMV beamformers eliminates the cross power P_c at the price of changing $P_{io} + P_{no}$ to $P_{i,B} + P_{n,B}$.

5. SIMULATION RESULTS

In this section, we present simulation results for confirmation and comparison. For all simulation examples, an eight-element ULA with inter-element spacing equal to half of the signal wavelength is considered. The numbers of Monte Carlo runs and data snapshots are set to 100. The background noise is spatially white and complex Gaussian with zero mean and unit variance. To evaluate the benefit of using \mathbf{B} for a LCMV beamformer, we define a gain factor which is the ratio of $SINR_B$ and $SINR_L$ given as follows:

$$G \equiv \frac{SINR_B}{SINR_L} = \frac{P_{io} + P_{no}}{P_{i,B} + P_{n,B}} + \frac{P_c}{P_{i,B} + P_{n,B}}. \quad (81)$$

When the blocking matrix is designed properly without enlarging $P_{io} + P_{no}$ too much, $P_{i,B} + P_{n,B}$ can be roughly approximated to $P_{io} + P_{no}$, especially when the cross power is dominant. Hence, (81) can be approximated by

$$G \equiv \frac{SINR_B}{SINR_L} \approx 1 + \frac{P_c}{P_{i,B} + P_{n,B}}. \quad (82)$$

Moreover, the theoretical results in (14) and (15) provided by [11] are also plotted for comparison.

Example 1: Three independent complex Gaussian sources are impinging on the array with direction angles $[11^\circ - 36^\circ 49^\circ]$ off array broadside and powers $[8 \ 20 \ 15]$ (dB), where the first one denotes the desired signal and the others the interferers. \mathbf{B} is set to the blocking matrix in [8] with order equal to 2 (i.e., $N = p - 2$). The theoretical results of (14), (15), (45), and (68) are plotted for comparison. Figures 4–6 show the output SINR, the related power terms derived in Sections 3 and 4, and the gain factor in dB of (81)–(82) versus the desired signal power. In Figure 4, it is seen that the curves of using (45) and (68) are close to those simulated by data snapshots and those of using (14) and (15), which explains the validity of the derivations and approximations. The output SINR without signal blocking sticks

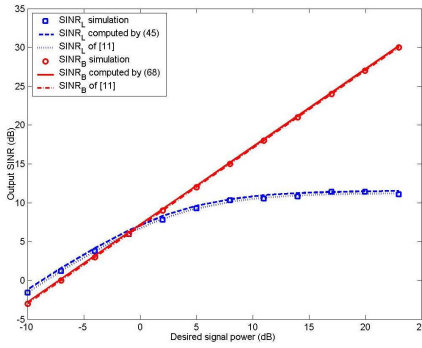


Figure 4. The output SINR versus desired signal power for *Example 1*.

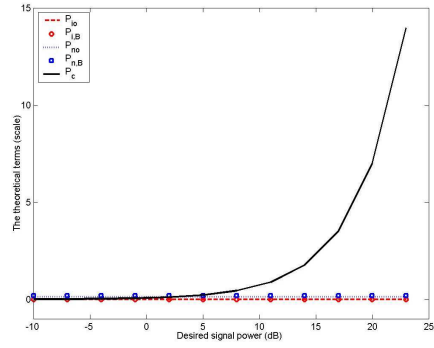


Figure 5. The theoretical terms versus desired signal power for *Example 1*.

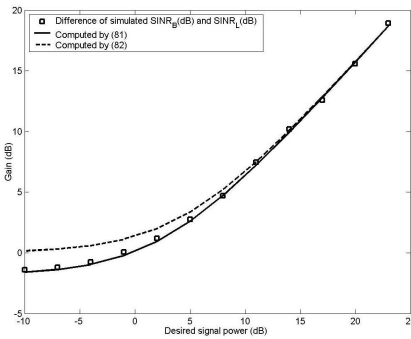


Figure 6. The gain factor of signal blocking versus desired signal power for *Example 1*.

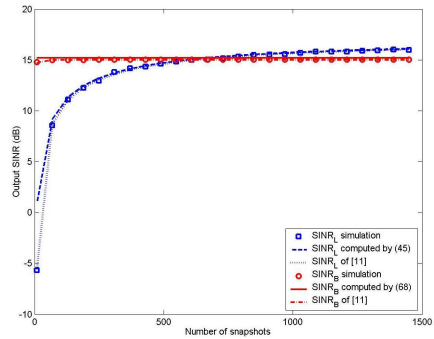


Figure 7. The output SINR versus number of data snapshots for *Example 1*.

to 12 dB even when the desired signal power is larger than 14 dB. In contrast, the output SINR with \mathbf{B} increases almost linearly as the desired signal power increases. This phenomenon can be seen from the results shown by Figure 5 where $P_{i,B}$ and $P_{n,B}$ do not vary with the desired signal power and approach P_{i0} and P_{n0} , respectively. However, P_c does increase as the desired signal power increases. In Figure 6, the gain of using signal blocking is smaller than zero for desired signal power smaller than -1 dB due to $P_{i0} + P_{n0} < P_{i,B} + P_{n,B}$. Since the cross power P_c increases with the growth of the desired signal power, its significance is also increased. When the desired signal power is stronger than -1 dB, $SINR_B$ starts transcending $SINR_L$ and the

gain factor in (81) is larger than 0 dB. For the desired signal power larger than 11 dB, the term $P_c/(P_{i,B} + P_{n,B})$ is dominant in (81), and the curves plotted by using (81) and (82) are almost the same. Next, we depict the output SINR, the related power terms derived in Sections 3 and 4, and the gain factor in dB of (81)–(82) versus the number of data snapshots for SNR = 8 dB in Figures 7–9, respectively. The simulated $SINR_B$ is almost invariant with the number of data snapshots in contrast to $SINR_L$ as expected. The scale of P_c is large and the gain of using signal blocking is substantial for data sample size smaller than 250. However, the scale of P_c becomes tiny and the

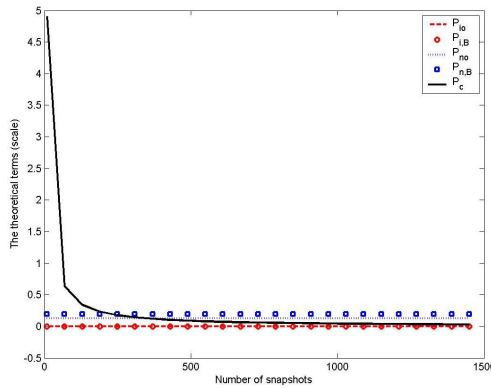


Figure 8. The theoretical terms versus number of data snapshots for *Example 1*.

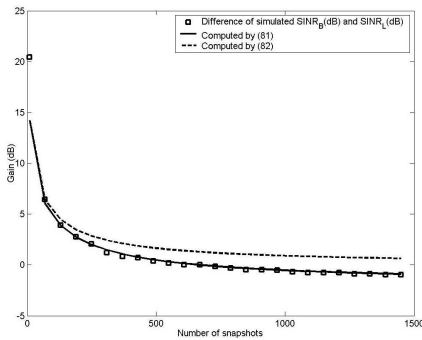


Figure 9. The gain factor of signal blocking versus number of data snapshots for *Example 1*.

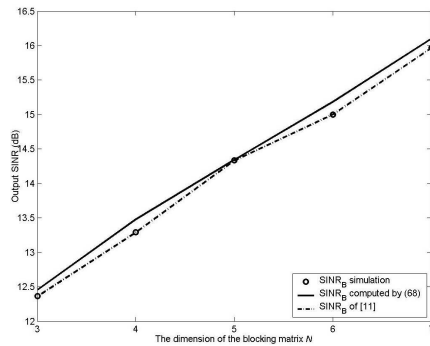


Figure 10. The output SINR versus dimension of the blocking matrix for *Example 1*.

output SINR without \mathbf{B} starts surpassing the one with \mathbf{B} when the number of snapshots is larger than about 750. To observe the effect of the dimension N of the blocking matrix on the system performance, the $SINR_B$ and the theoretical terms $P_{i,B}$ and $P_{n,B}$ with varying N are depicted in Figures 10 and 11, respectively. Notice that the proposed formula of (68) still predicts the simulated output SINR well. As we see from Figure 10, the output SINR is increased with the growth of N because the DOF for adaptive beamforming is also increased. Since more DOF is beneficial to eliminating the noise component, the $P_{n,B}$ is decreasing in Figure 11, while the $P_{i,B}$ is tiny and almost invariant with N . In spite of the loss of DOF, increasing the order of the blocking matrix may alleviate the performance degradation due to steering angle error [8].

Example 2: Here, seven independent BPSK signals with bipolar rectangular waveforms are considered for the case of $q > 3$. The direction angles and the powers of the sources are $[11^\circ -36^\circ 49^\circ -55^\circ 32^\circ 78^\circ -64^\circ]$ off array broadside and $[8 20 15 10 8 3 5]$ (dB), respectively, where the first one denotes the desired signal. The blocking matrix of (70) is used, and the theoretical results of (48) and (80) are plotted instead of (45) and (68), respectively. First, the output SINRs versus the number of signal sources are shown in Figure 12 for the number of elements equal to 8 and 16, respectively. The differences between the theoretical results and the simulated ones are all within 1 dB. This confirms the accuracy of the closed-forms given in (48) and (80). Considering the $SINR_B$ for $p = 8$, we note that the errors between the theoretical results and the simulated ones are more significant for higher q 's. However, the errors become smaller when the

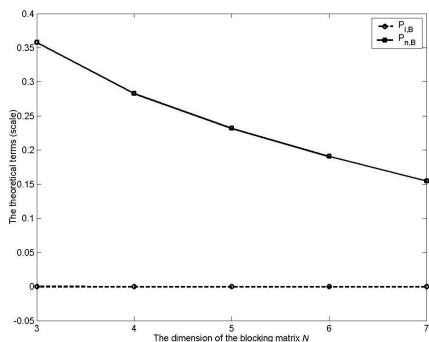


Figure 11. The theoretical terms versus dimension of the blocking matrix for *Example 1*.

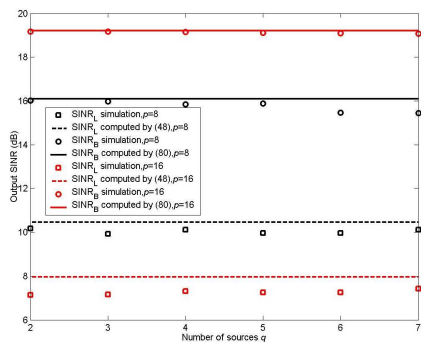


Figure 12. The output SINR versus number of sources for *Example 2*.

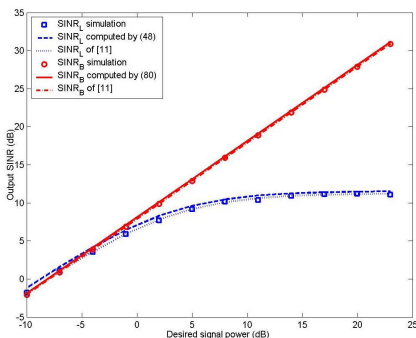


Figure 13. The output SINR versus desired signal power for *Example 2*.

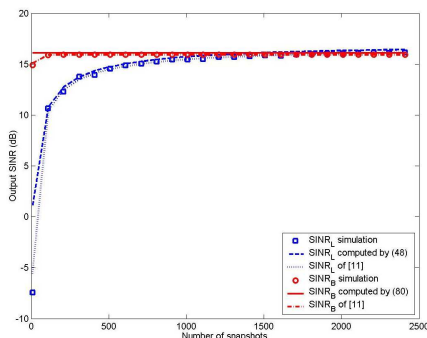


Figure 14. The output SINR versus number of data snapshots for *Example 2*.

number of elements is increased to 16 because the assumptions $|d_{ij}|^2 \ll 1$ and $|d_{ij,B}|^2 \ll 1$ become more reasonable. On the other hand, the prediction errors for the $SINR_L$ are almost uncorrelated with q . Comparing the $SINR_L$ for $p = 8$ and $p = 16$, we observe that the overall errors are increased when the number of elements is doubled. Because P_{io} and P_{no} are usually much smaller than P_c for deficient sample size, the approximations for generalizing P_{io} and P_{no} to the case with multiple interferers are relative marginal. The errors for the $SINR_L$ are mainly due to the approximation used in (19) which is valid when $m/p > 3$. Since the ratio m/p becomes smaller when p is doubled, the theoretical results of $p = 8$ are more accurate than those of $p = 16$ as expected.

Next, we consider the 8-element array impinged by the first five signal sources (i.e., $q = 5$) mentioned above. The output SINR versus the desired signal power using 100 data snapshots and the output SINR versus the number of snapshots for $SNR = 8$ dB are presented in Figures 13 and 14, respectively. The reason for the performance difference between LCMV beamformers with \mathbf{B} and without \mathbf{B} is similar to that discussed in *Example 1*. As shown in Figures 13 and 4, the difference between $SINR_B$ and $SINR_L$ for $\sigma_{s1}^2 < -4$ dB (i.e., P_c is weak) becomes smaller. This is due to the increase of one DOF when the order of \mathbf{B} is reduced from 2 to 1. The results computed by (48) and (80) are still close to those of simulation and those computed by (14) and (15) for $q = 5$. Again, we observe that the validity of the theoretical work is confirmed in this case.

6. CONCLUSION

This paper has analyzed the finite data performance of LCMV beamformers with and without signal blocking. The presented formulas are more comprehensive than the existing formulas in the literature and provide insights into the effect of using signal blocking. Based on the analytical formulas, we can see that the signal blocking operation does not only block the desired signal but also eliminates the cross weight component caused by the correlation due to finite data samples. This provides the detailed explanation to the fact that a LCMV beamformer with signal blocking converges faster than the same beamformer without signal blocking, especially when the number of array elements or the desired signal power is large. Furthermore, the explicit formulas have been extended to a general situation with one desired signal and multiple interferers. The validity of the theoretical work is confirmed by simulations. The extension of our theoretical work to the case with broadband signal sources is currently under investigation.

APPENDIX A.

Here, we apply the well-known mathematical induction [18,19] to prove (48) is a reasonable approximated result of (32) after expanding \mathbf{Q} . First, substituting $q = 2$ into (48) yields the result of (46), which is shown to be true in Section 3.3. Next, we suppose that (32) can be derived and simplified to (48) for $q = r$. Then, we have

$$P_{io(r)} = \sum_{k=2}^r \sigma_{sk}^2 \left| \frac{\mathbf{a}_1^H \mathbf{Q}_{(r)}^{-1} \mathbf{a}_k}{\mathbf{a}_1^H \mathbf{Q}_{(r)}^{-1} \mathbf{a}_1} \right|^2 \approx \sum_{k=2}^r \frac{\sigma_{sk}^2 \sigma_n^4 |d_{1k}|^2}{(\sigma_n^2 + p\sigma_{sk}^2)^2} \quad (\text{A1})$$

and

$$P_{no(r)} = \sigma_n^2 \frac{\left\| \mathbf{Q}_{(r)}^{-1} \mathbf{a}_1 \right\|^2}{\left(\mathbf{a}_1^H \mathbf{Q}_{(r)}^{-1} \mathbf{a}_1 \right)^2} \approx \frac{\sigma_n^2}{p}, \quad (\text{A2})$$

where the subscript (r) denotes the particular case of $q = r$. Based on (A1) and (A2), we then show that the output SINR of (48) can be derived from (32) under $q = r + 1$.

Since the analysis in Section 3.1 is suitable for a general q , we

apply (23) to obtain the P_{io} for $q = r + 1$ as follows:

$$\begin{aligned}
 P_{io(r+1)} &= \sum_{k=2}^{r+1} \sigma_{sk}^2 \left| \frac{\mathbf{a}_1^H \mathbf{Q}_{(r+1)}^{-1} \mathbf{a}_k}{\mathbf{a}_1^H \mathbf{Q}_{(r+1)}^{-1} \mathbf{a}_1} \right|^2 \\
 &= \sum_{k=2}^r \sigma_{sk}^2 \left| \frac{\mathbf{a}_1^H \mathbf{Q}_{(r+1)}^{-1} \mathbf{a}_k}{\mathbf{a}_1^H \mathbf{Q}_{(r+1)}^{-1} \mathbf{a}_1} \right|^2 + \sigma_{s(r+1)}^2 \left| \frac{\mathbf{a}_1^H \mathbf{Q}_{(r+1)}^{-1} \mathbf{a}_{r+1}}{\mathbf{a}_1^H \mathbf{Q}_{(r+1)}^{-1} \mathbf{a}_1} \right|^2. \quad (A3)
 \end{aligned}$$

Using the recursive formula of \mathbf{Q}^{-1} in (35), we have

$$\mathbf{Q}_{(r+1)}^{-1} = \mathbf{Q}_{(r)}^{-1} \left(\mathbf{I} - \frac{\mathbf{a}_{r+1} \mathbf{a}_{r+1}^H \mathbf{Q}_{(r)}^{-1}}{\sigma_{s(r+1)}^{-2} + \mathbf{a}_{r+1}^H \mathbf{Q}_{(r)}^{-1} \mathbf{a}_{r+1}} \right). \quad (A4)$$

From (A4), we obtain

$$\mathbf{a}_1^H \mathbf{Q}_{(r+1)}^{-1} \mathbf{a}_1 = \mathbf{a}_1^H \mathbf{Q}_{(r)}^{-1} \mathbf{a}_1 - \frac{\mathbf{a}_1^H \mathbf{Q}_{(r)}^{-1} \mathbf{a}_{r+1} \mathbf{a}_{r+1}^H \mathbf{Q}_{(r)}^{-1} \mathbf{a}_1}{\sigma_{s(r+1)}^{-2} + \mathbf{a}_{r+1}^H \mathbf{Q}_{(r)}^{-1} \mathbf{a}_{r+1}} \quad (A5)$$

and

$$\mathbf{a}_1^H \mathbf{Q}_{(r+1)}^{-1} \mathbf{a}_k = \mathbf{a}_1^H \mathbf{Q}_{(r)}^{-1} \mathbf{a}_k - \frac{\mathbf{a}_1^H \mathbf{Q}_{(r)}^{-1} \mathbf{a}_{r+1} \mathbf{a}_{r+1}^H \mathbf{Q}_{(r)}^{-1} \mathbf{a}_k}{\sigma_{s(r+1)}^{-2} + \mathbf{a}_{r+1}^H \mathbf{Q}_{(r)}^{-1} \mathbf{a}_{r+1}}. \quad (A6)$$

Now, consider the optimal weight vector $\mathbf{w}_{o1} = \mathbf{Q}_{(r)}^{-1} \mathbf{a}_1$ without the normalized scalar. Since $\mathbf{Q}_{(r)}$ contains the 2nd to r th signal sources, the directions of \mathbf{a}_1 , \mathbf{a}_{r+1} , and \mathbf{a}_k , $k = 2, 3, \dots, r$, are regarded as the desired signal, noise, and interference, respectively. The responses of \mathbf{w}_{o1} in the three directions are different and in general, $\mathbf{w}_{o1}^H \mathbf{a}_1 \gg \mathbf{w}_{o1}^H \mathbf{a}_{r+1} \gg \mathbf{w}_{o1}^H \mathbf{a}_k$. That is,

$$\mathbf{a}_1^H \mathbf{Q}_{(r)}^{-1} \mathbf{a}_1 \gg \mathbf{a}_1^H \mathbf{Q}_{(r)}^{-1} \mathbf{a}_{r+1} \gg \mathbf{a}_1^H \mathbf{Q}_{(r)}^{-1} \mathbf{a}_k. \quad (A7)$$

On the other hand, if the steering vector of the desired signal becomes \mathbf{a}_{r+1} , the according optimal weight vector is $\mathbf{w}_{o2} = \mathbf{Q}_{(r)}^{-1} \mathbf{a}_{r+1}$. As to \mathbf{w}_{o2} , the directions of \mathbf{a}_1 , \mathbf{a}_{r+1} , and \mathbf{a}_k are identified as the noise, desired signal, and interference, respectively. Similarly, we have

$$\mathbf{a}_{r+1}^H \mathbf{Q}_{(r)}^{-1} \mathbf{a}_{r+1} \gg \mathbf{a}_{r+1}^H \mathbf{Q}_{(r)}^{-1} \mathbf{a}_1 \gg \mathbf{a}_{r+1}^H \mathbf{Q}_{(r)}^{-1} \mathbf{a}_k. \quad (A8)$$

Note that (A7) and (A8) hold because the 1st and $(r + 1)$ th sources are excluded from $\mathbf{Q}_{(r)}$ and all the $(r + 1)$ sources are assumed to be separate enough so that $|d_{ij}|^2 \ll 1$, $i \neq j$. Combining (A7) and (A8) yields

$$\begin{aligned}
 \mathbf{a}_1^H \mathbf{Q}_{(r)}^{-1} \mathbf{a}_1 &\approx \mathbf{a}_{r+1}^H \mathbf{Q}_{(r)}^{-1} \mathbf{a}_{r+1} \gg \mathbf{a}_1^H \mathbf{Q}_{(r)}^{-1} \mathbf{a}_{r+1} \\
 &\approx \mathbf{a}_{r+1}^H \mathbf{Q}_{(r)}^{-1} \mathbf{a}_1 \gg \mathbf{a}_1^H \mathbf{Q}_{(r)}^{-1} \mathbf{a}_k \approx \mathbf{a}_{r+1}^H \mathbf{Q}_{(r)}^{-1} \mathbf{a}_k. \quad (A9)
 \end{aligned}$$

According to (A9), $\mathbf{a}_1^H \mathbf{Q}_{(r+1)}^{-1} \mathbf{a}_1$ in (A5) and $\mathbf{a}_1^H \mathbf{Q}_{(r+1)}^{-1} \mathbf{a}_k$ in (A6) can be approximated as follows:

$$\mathbf{a}_1^H \mathbf{Q}_{(r+1)}^{-1} \mathbf{a}_1 \approx \mathbf{a}_1^H \mathbf{Q}_{(r)}^{-1} \mathbf{a}_1 \quad (\text{A10})$$

and

$$\mathbf{a}_1^H \mathbf{Q}_{(r+1)}^{-1} \mathbf{a}_k \approx \mathbf{a}_1^H \mathbf{Q}_{(r)}^{-1} \mathbf{a}_k, \quad (\text{A11})$$

respectively. Using (A1), (A10), and (A11), the summation term on the right-hand side of (A3) can be approximated as follows:

$$\sum_{k=2}^r \sigma_{sk}^2 \left| \frac{\mathbf{a}_1^H \mathbf{Q}_{(r+1)}^{-1} \mathbf{a}_k}{\mathbf{a}_1^H \mathbf{Q}_{(r+1)}^{-1} \mathbf{a}_1} \right|^2 \approx \sum_{k=2}^r \sigma_{sk}^2 \left| \frac{\mathbf{a}_1^H \mathbf{Q}_{(r)}^{-1} \mathbf{a}_k}{\mathbf{a}_1^H \mathbf{Q}_{(r)}^{-1} \mathbf{a}_1} \right|^2 \approx \sum_{k=2}^r \frac{\sigma_{sk}^2 \sigma_n^4 |d_{1k}|^2}{(\sigma_n^2 + p\sigma_{sk}^2)^2}. \quad (\text{A12})$$

Further, applying the results of (A10) and (A11), we have

$$\mathbf{a}_1^H \mathbf{Q}_{(r+1)}^{-1} \mathbf{a}_1 \approx \mathbf{a}_1^H \dot{\mathbf{Q}}_{(r)}^{-1} \mathbf{a}_1 \quad (\text{A13})$$

and

$$\mathbf{a}_1^H \mathbf{Q}_{(r+1)}^{-1} \mathbf{a}_{r+1} \approx \mathbf{a}_1^H \dot{\mathbf{Q}}_{(r)}^{-1} \mathbf{a}_{r+1}, \quad (\text{A14})$$

where $\dot{\mathbf{Q}}_{(r)}$ is obtained by removing one of the 2nd to r th sources from $\mathbf{Q}_{(r+1)}$. Analogous to each term of (A12), the second term on the right-hand side of (A3) can be derived to

$$\begin{aligned} \sigma_{s(r+1)}^2 \left| \frac{\mathbf{a}_1^H \mathbf{Q}_{(r+1)}^{-1} \mathbf{a}_{r+1}}{\mathbf{a}_1^H \mathbf{Q}_{(r+1)}^{-1} \mathbf{a}_1} \right|^2 &\approx \sigma_{s(r+1)}^2 \left| \frac{\mathbf{a}_1^H \dot{\mathbf{Q}}_{(r)}^{-1} \mathbf{a}_{r+1}}{\mathbf{a}_1^H \dot{\mathbf{Q}}_{(r)}^{-1} \mathbf{a}_1} \right|^2 \\ &\approx \frac{\sigma_{s(r+1)}^2 \sigma_n^4 |d_{1(r+1)}|^2}{(\sigma_n^2 + p\sigma_{s(r+1)}^2)^2}. \end{aligned} \quad (\text{A15})$$

It follows from (A12) and (A15) that P_{io} under $q = r + 1$ is given by

$$P_{io(r+1)} = \sum_{k=2}^{r+1} \sigma_{sk}^2 \left| \frac{\mathbf{a}_1^H \mathbf{Q}_{(r+1)}^{-1} \mathbf{a}_k}{\mathbf{a}_1^H \mathbf{Q}_{(r+1)}^{-1} \mathbf{a}_1} \right|^2 \approx \sum_{k=2}^{r+1} \frac{\sigma_{sk}^2 \sigma_n^4 |d_{1k}|^2}{(\sigma_n^2 + p\sigma_{sk}^2)^2}. \quad (\text{A16})$$

Next, consider the P_{no} in (28) for $q = r + 1$ as follows:

$$P_{no(r+1)} = \sigma_n^2 \frac{\left\| \mathbf{Q}_{(r+1)}^{-1} \mathbf{a}_1 \right\|^2}{\left(\mathbf{a}_1^H \mathbf{Q}_{(r+1)}^{-1} \mathbf{a}_1 \right)^2}, \quad (\text{A17})$$

where the squared norm of $\mathbf{Q}_{(r+1)}^{-1} \mathbf{a}_1$ can be derived to

$$\begin{aligned} \left\| \mathbf{Q}_{(r+1)}^{-1} \mathbf{a}_1 \right\|^2 = & \left\| \mathbf{Q}_{(r)}^{-1} \mathbf{a}_1 \right\|^2 + \left| \frac{\mathbf{a}_{r+1}^H \mathbf{Q}_{(r)}^{-1} \mathbf{a}_1}{\sigma_{s(r+1)}^{-2} + \mathbf{a}_{r+1}^H \mathbf{Q}_{(r)}^{-1} \mathbf{a}_{r+1}} \right|^2 \left\| \mathbf{Q}_{(r)}^{-1} \mathbf{a}_{r+1} \right\|^2 \\ & - 2\text{Re} \left(\frac{\mathbf{a}_{r+1}^H \mathbf{Q}_{(r)}^{-1} \mathbf{a}_1}{\sigma_{s(r+1)}^{-2} + \mathbf{a}_{r+1}^H \mathbf{Q}_{(r)}^{-1} \mathbf{a}_{r+1}} \mathbf{a}_1^H \mathbf{Q}_{(r)}^{-1} \mathbf{Q}_{(r)}^{-1} \mathbf{a}_{r+1} \right) \end{aligned} \quad (\text{A18})$$

according to (A4). Again, utilizing the relationship of (A9), Eq. (A18) can be approximated to

$$\left\| \mathbf{Q}_{(r+1)}^{-1} \mathbf{a}_1 \right\|^2 \approx \left\| \mathbf{Q}_{(r)}^{-1} \mathbf{a}_1 \right\|^2. \quad (\text{A19})$$

Substituting (A19) and (A10) into (A17) and utilizing (A2) yields

$$P_{no(r+1)} = \sigma_n^2 \frac{\left\| \mathbf{Q}_{(r+1)}^{-1} \mathbf{a}_1 \right\|^2}{\left(\mathbf{a}_1^H \mathbf{Q}_{(r+1)}^{-1} \mathbf{a}_1 \right)^2} \approx \sigma_n^2 \frac{\left\| \mathbf{Q}_{(r)}^{-1} \mathbf{a}_1 \right\|^2}{\left(\mathbf{a}_1^H \mathbf{Q}_{(r)}^{-1} \mathbf{a}_1 \right)^2} \approx \frac{\sigma_n^2}{p}. \quad (\text{A20})$$

From the P_{io} in (A16) and P_{no} in (A20), we have the output SINR for $q = r + 1$ given by

$$SINR_{L(r+1)} \approx \frac{\sigma_{s1}^2}{\sum_{k=2}^{r+1} \frac{\sigma_{sk}^2 \sigma_n^4 |d_{1k}|^2}{(\sigma_n^2 + p\sigma_{sk}^2)^2} + \frac{\sigma_n^2}{p} + \frac{(p-1)\sigma_{s1}^2}{m}}, \quad (\text{A21})$$

which is the same as (48) with q replaced by $r + 1$. Therefore, it is proved by mathematical induction that the approximated $SINR_L$ in (48) is valid for $2 \leq q < p$. Since the approximated error exists in each stage of the recursive expression, the proposed formula in (48) may be inaccurate for greater q due to error propagation. However, our experiment in Section 5 shows that the errors are acceptable even if $q = p - 1$.

APPENDIX B.

In this appendix, we apply the mathematical induction [18,19] to prove (69) is a reasonable approximated result of (54) after expanding \mathbf{Q}_B , where the blocking matrix \mathbf{B} possesses the properties of (10) and (59). First, substituting $q = 2$ into (69) yields

$$\begin{aligned} SINR_B \approx & \frac{\sigma_{s1}^2}{\frac{\sigma_{s2}^2 \sigma_n^4 \bar{\mathbf{a}}_2^H (\mathbf{B}\mathbf{B}^H)^{-1} \bar{\mathbf{a}}_2 |d_{12,B}|^2}{\bar{\mathbf{a}}_1^H (\mathbf{B}\mathbf{B}^H)^{-1} \bar{\mathbf{a}}_1 \left[\sigma_n^2 + |\gamma_2|^2 \sigma_{s2}^2 \bar{\mathbf{a}}_2^H (\mathbf{B}\mathbf{B}^H)^{-1} \bar{\mathbf{a}}_2 \right]^2} + \sigma_n^2 \frac{\bar{\mathbf{a}}_1^H (\mathbf{B}\mathbf{B}^H)^{-1} (\mathbf{B}\mathbf{B}^H)^{-1} \bar{\mathbf{a}}_1}{\left[\bar{\mathbf{a}}_1^H (\mathbf{B}\mathbf{B}^H)^{-1} \bar{\mathbf{a}}_1 \right]^2}}. \end{aligned} \quad (\text{B1})$$

Since (B1) is a special case of (68), the result of (69) is true for $q = 2$. Assume that (54) can be derived and simplified to (69) for $q = r$. Then, we have

$$P_{i,B(r)} \approx \sum_{k=2}^r \sigma_{sk}^2 \left| \frac{\bar{\mathbf{a}}_1^H \mathbf{Q}_{B(r)}^{-1} \bar{\mathbf{a}}_k}{\bar{\mathbf{a}}_1^H \mathbf{Q}_{B(r)}^{-1} \bar{\mathbf{a}}_1} \right|^2$$

$$\approx \sum_{k=2}^r \frac{\sigma_{sk}^2 \sigma_n^4 \bar{\mathbf{a}}_k^H (\mathbf{B}\mathbf{B}^H)^{-1} \bar{\mathbf{a}}_k |d_{1k,B}|^2}{\bar{\mathbf{a}}_1^H (\mathbf{B}\mathbf{B}^H)^{-1} \bar{\mathbf{a}}_1 \left[\sigma_n^2 + |\gamma_{kl}|^2 \sigma_{sk}^2 \bar{\mathbf{a}}_k^H (\mathbf{B}\mathbf{B}^H)^{-1} \bar{\mathbf{a}}_k \right]^2} \quad (\text{B2})$$

$$P_{n,B(r)} \approx \sigma_n^2 \frac{\left\| \mathbf{Q}_{B(r)}^{-1} \bar{\mathbf{a}}_1 \right\|^2}{\left(\bar{\mathbf{a}}_1^H \mathbf{Q}_{B(r)}^{-1} \bar{\mathbf{a}}_1 \right)^2} \approx \sigma_n^2 \frac{\bar{\mathbf{a}}_1^H (\mathbf{B}\mathbf{B}^H)^{-1} (\mathbf{B}\mathbf{B}^H)^{-1} \bar{\mathbf{a}}_1}{\left[\bar{\mathbf{a}}_1^H (\mathbf{B}\mathbf{B}^H)^{-1} \bar{\mathbf{a}}_1 \right]^2}, \quad (\text{B3})$$

where the subscript (r) denotes the particular case of $q = r$. Based on (B2) and (B3), we then show that the output SINR of (69) can also be derived from (54) under $q = r + 1$. It follows from (52) that the $P_{i,B}$ for $q = r + 1$ is approximately given by

$$P_{i,B(r+1)} \approx \sum_{k=2}^{r+1} \sigma_{sk}^2 \left| \frac{\bar{\mathbf{a}}_1^H \mathbf{Q}_{B(r+1)}^{-1} \bar{\mathbf{a}}_k}{\bar{\mathbf{a}}_1^H \mathbf{Q}_{B(r+1)}^{-1} \bar{\mathbf{a}}_1} \right|^2$$

$$= \sum_{k=2}^r \sigma_{sk}^2 \left| \frac{\bar{\mathbf{a}}_1^H \mathbf{Q}_{B(r+1)}^{-1} \bar{\mathbf{a}}_k}{\bar{\mathbf{a}}_1^H \mathbf{Q}_{B(r+1)}^{-1} \bar{\mathbf{a}}_1} \right|^2 + \sigma_{s(r+1)}^2 \left| \frac{\bar{\mathbf{a}}_1^H \mathbf{Q}_{B(r+1)}^{-1} \bar{\mathbf{a}}_{r+1}}{\bar{\mathbf{a}}_1^H \mathbf{Q}_{B(r+1)}^{-1} \bar{\mathbf{a}}_1} \right|^2. \quad (\text{B4})$$

Using the recursive formula of \mathbf{Q}_B^{-1} in (57), we have

$$\mathbf{Q}_{B(r+1)}^{-1} = \mathbf{Q}_{B(r)}^{-1} \left(\mathbf{I} - \frac{\mathbf{B}\mathbf{a}_{r+1}\mathbf{a}_{r+1}^H\mathbf{B}^H\mathbf{Q}_{B(r)}^{-1}}{\sigma_{s(r+1)}^{-2} + \mathbf{a}_{r+1}^H\mathbf{B}^H\mathbf{Q}_{B(r)}^{-1}\mathbf{B}\mathbf{a}_{r+1}} \right). \quad (\text{B5})$$

Pre-multiplying $\bar{\mathbf{a}}_1^H$ and post-multiplying $\bar{\mathbf{a}}_1$ and $\bar{\mathbf{a}}_k$, $k = 2, 3, \dots, r$, to $\mathbf{Q}_{B(r+1)}^{-1}$, we obtain

$$\bar{\mathbf{a}}_1^H \mathbf{Q}_{B(r+1)}^{-1} \bar{\mathbf{a}}_1 = \bar{\mathbf{a}}_1^H \mathbf{Q}_{B(r)}^{-1} \bar{\mathbf{a}}_1 - \frac{\bar{\mathbf{a}}_1^H \mathbf{Q}_{B(r)}^{-1} \mathbf{B}\mathbf{a}_{r+1}\mathbf{a}_{r+1}^H\mathbf{B}^H\mathbf{Q}_{B(r)}^{-1} \bar{\mathbf{a}}_1}{\sigma_{s(r+1)}^{-2} + \mathbf{a}_{r+1}^H\mathbf{B}^H\mathbf{Q}_{B(r)}^{-1}\mathbf{B}\mathbf{a}_{r+1}} \quad (\text{B6})$$

and

$$\bar{\mathbf{a}}_1^H \mathbf{Q}_{B(r+1)}^{-1} \bar{\mathbf{a}}_k = \bar{\mathbf{a}}_1^H \mathbf{Q}_{B(r)}^{-1} \bar{\mathbf{a}}_k - \frac{\bar{\mathbf{a}}_1^H \mathbf{Q}_{B(r)}^{-1} \mathbf{B}\mathbf{a}_{r+1}\mathbf{a}_{r+1}^H\mathbf{B}^H\mathbf{Q}_{B(r)}^{-1} \bar{\mathbf{a}}_k}{\sigma_{s(r+1)}^{-2} + \mathbf{a}_{r+1}^H\mathbf{B}^H\mathbf{Q}_{B(r)}^{-1}\mathbf{B}\mathbf{a}_{r+1}}. \quad (\text{B7})$$

For the weight vector $\mathbf{w}_{B1} = \mathbf{Q}_{B(r)}^{-1} \bar{\mathbf{a}}_1$, the directions of $\bar{\mathbf{a}}_1$, $\mathbf{B}\mathbf{a}_{r+1}$ ($= \gamma_{r+1} \bar{\mathbf{a}}_{r+1}$), and $\bar{\mathbf{a}}_k$ are respectively regarded as the desired signal, noise, and interference, respectively. On the other hand, for the weight vector $\mathbf{w}_{B2} = \mathbf{Q}_{B(r)}^{-1} \mathbf{B}\mathbf{a}_{r+1}$, the directions of $\bar{\mathbf{a}}_1$, $\mathbf{B}\mathbf{a}_{r+1}$, and $\bar{\mathbf{a}}_k$ are regarded as the noise, desired signal, and interference, respectively. Similar to (A7)–(A9), we obtain the following relationships:

$$\begin{aligned} \bar{\mathbf{a}}_1^H \mathbf{Q}_{B(r)}^{-1} \bar{\mathbf{a}}_1 &\approx \mathbf{a}_{r+1}^H \mathbf{B}^H \mathbf{Q}_{B(r)}^{-1} \mathbf{B}\mathbf{a}_{r+1} \gg \bar{\mathbf{a}}_1^H \mathbf{Q}_{B(r)}^{-1} \mathbf{B}\mathbf{a}_{r+1} \\ &\approx \mathbf{a}_{r+1}^H \mathbf{B}^H \mathbf{Q}_{B(r)}^{-1} \bar{\mathbf{a}}_1 \gg \bar{\mathbf{a}}_1^H \mathbf{Q}_{B(r)}^{-1} \bar{\mathbf{a}}_k \approx \mathbf{a}_{r+1}^H \mathbf{B}^H \mathbf{Q}_{B(r)}^{-1} \bar{\mathbf{a}}_k. \end{aligned} \quad (\text{B8})$$

Note that (B8) is valid when all the $(r + 1)$ sources are assumed to be separate enough so that $|d_{ij,B}|^2 \ll 1$ for $i \neq j$. According to (B8), the $\bar{\mathbf{a}}_1^H \mathbf{Q}_{B(r+1)}^{-1} \bar{\mathbf{a}}_1$ in (B6) and $\bar{\mathbf{a}}_1^H \mathbf{Q}_{B(r+1)}^{-1} \bar{\mathbf{a}}_k$ in (B7) can be approximated to

$$\bar{\mathbf{a}}_1^H \mathbf{Q}_{B(r+1)}^{-1} \bar{\mathbf{a}}_1 \approx \bar{\mathbf{a}}_1^H \mathbf{Q}_{B(r)}^{-1} \bar{\mathbf{a}}_1 \quad (\text{B9})$$

and

$$\bar{\mathbf{a}}_1^H \mathbf{Q}_{B(r+1)}^{-1} \bar{\mathbf{a}}_k \approx \bar{\mathbf{a}}_1^H \mathbf{Q}_{B(r)}^{-1} \bar{\mathbf{a}}_k, \quad (\text{B10})$$

respectively. Using (B2), (B9), and (B10), the summation term in (B4) can be approximated to

$$\begin{aligned} &\sum_{k=2}^r \sigma_{sk}^2 \left| \frac{\bar{\mathbf{a}}_1^H \mathbf{Q}_{B(r+1)}^{-1} \bar{\mathbf{a}}_k}{\bar{\mathbf{a}}_1^H \mathbf{Q}_{B(r+1)}^{-1} \bar{\mathbf{a}}_1} \right|^2 \approx \sum_{k=2}^r \sigma_{sk}^2 \left| \frac{\bar{\mathbf{a}}_1^H \mathbf{Q}_{B(r)}^{-1} \bar{\mathbf{a}}_k}{\bar{\mathbf{a}}_1^H \mathbf{Q}_{B(r)}^{-1} \bar{\mathbf{a}}_1} \right|^2 \\ &\approx \sum_{k=2}^r \frac{\sigma_{sk}^2 \sigma_n^4 \bar{\mathbf{a}}_k^H (\mathbf{B}\mathbf{B}^H)^{-1} \bar{\mathbf{a}}_k |d_{1k,B}|^2}{\bar{\mathbf{a}}_1^H (\mathbf{B}\mathbf{B}^H)^{-1} \bar{\mathbf{a}}_1 [\sigma_n^2 + |\gamma_k|^2 \sigma_{sk}^2 \bar{\mathbf{a}}_k^H (\mathbf{B}\mathbf{B}^H)^{-1} \bar{\mathbf{a}}_k]}^2. \end{aligned} \quad (\text{B11})$$

Further, applying the results of (B9) and (B10), we have

$$\bar{\mathbf{a}}_1^H \mathbf{Q}_{B(r+1)}^{-1} \bar{\mathbf{a}}_1 \approx \bar{\mathbf{a}}_1^H \dot{\mathbf{Q}}_{B(r)}^{-1} \bar{\mathbf{a}}_1 \quad (\text{B12})$$

and

$$\bar{\mathbf{a}}_1^H \mathbf{Q}_{B(r+1)}^{-1} \bar{\mathbf{a}}_{r+1} \approx \bar{\mathbf{a}}_1^H \dot{\mathbf{Q}}_{B(r)}^{-1} \bar{\mathbf{a}}_{r+1}, \quad (\text{B13})$$

where $\dot{\mathbf{Q}}_{B(r)}$ is obtained by removing one of the 2nd to r th sources from $\mathbf{Q}_{B(r+1)}$. Analogous to each term of (B11), the second term of (B4) can be derived to

$$\begin{aligned} &\sigma_{s(r+1)}^2 \left| \frac{\bar{\mathbf{a}}_1^H \mathbf{Q}_{B(r+1)}^{-1} \bar{\mathbf{a}}_{r+1}}{\bar{\mathbf{a}}_1^H \mathbf{Q}_{B(r+1)}^{-1} \bar{\mathbf{a}}_1} \right|^2 \approx \sigma_{s(r+1)}^2 \left| \frac{\bar{\mathbf{a}}_1^H \dot{\mathbf{Q}}_{B(r)}^{-1} \bar{\mathbf{a}}_{r+1}}{\bar{\mathbf{a}}_1^H \dot{\mathbf{Q}}_{B(r)}^{-1} \bar{\mathbf{a}}_1} \right|^2 \\ &\approx \frac{\sigma_{s(r+1)}^2 \sigma_n^4 \bar{\mathbf{a}}_{r+1}^H (\mathbf{B}\mathbf{B}^H)^{-1} \bar{\mathbf{a}}_{r+1} |d_{1(r+1),B}|^2}{\bar{\mathbf{a}}_1^H (\mathbf{B}\mathbf{B}^H)^{-1} \bar{\mathbf{a}}_1 [\sigma_n^2 + |\gamma_{r+1}|^2 \sigma_{s(r+1)}^2 \bar{\mathbf{a}}_{r+1}^H (\mathbf{B}\mathbf{B}^H)^{-1} \bar{\mathbf{a}}_{r+1}]}^2. \end{aligned} \quad (\text{B14})$$

It follows from (B11) and (B14) that $P_{i,B}$ under $q = r + 1$ is given by

$$P_{i,B(r+1)} \approx \sum_{k=2}^{r+1} \frac{\sigma_{sk}^2 \sigma_n^4 \bar{\mathbf{a}}_k^H (\mathbf{B}\mathbf{B}^H)^{-1} \bar{\mathbf{a}}_k |d_{1k,B}|^2}{\bar{\mathbf{a}}_1^H (\mathbf{B}\mathbf{B}^H)^{-1} \bar{\mathbf{a}}_1 [\sigma_n^2 + |\gamma_k|^2 \sigma_{sk}^2 \bar{\mathbf{a}}_k^H (\mathbf{B}\mathbf{B}^H)^{-1} \bar{\mathbf{a}}_k]}^2. \quad (\text{B15})$$

Next, consider the $P_{n,B}$ in (53) for $q = r + 1$ as follows:

$$P_{n,B(r+1)} \approx \sigma_n^2 \frac{\left\| \mathbf{Q}_{B(r+1)}^{-1} \bar{\mathbf{a}}_1 \right\|^2}{\left(\bar{\mathbf{a}}_1^H \mathbf{Q}_{B(r+1)}^{-1} \bar{\mathbf{a}}_1 \right)^2}, \quad (\text{B16})$$

where the squared norm of $\mathbf{Q}_{B(r+1)}^{-1} \bar{\mathbf{a}}_1$ can be derived to

$$\begin{aligned} & \left\| \mathbf{Q}_{B(r+1)}^{-1} \bar{\mathbf{a}}_1 \right\|^2 \\ &= \left\| \mathbf{Q}_{B(r)}^{-1} \bar{\mathbf{a}}_1 \right\|^2 + \left| \frac{\mathbf{a}_{r+1}^H \mathbf{B}^H \mathbf{Q}_{B(r)}^{-1} \bar{\mathbf{a}}_1}{\sigma_{s(r+1)}^{-2} + \mathbf{a}_{r+1}^H \mathbf{B}^H \mathbf{Q}_{B(r)}^{-1} \mathbf{B} \mathbf{a}_{r+1}} \right|^2 \left\| \mathbf{Q}_{B(r)}^{-1} \mathbf{B} \mathbf{a}_{r+1} \right\|^2 \\ & \quad - 2\text{Re} \left(\frac{\mathbf{a}_{r+1}^H \mathbf{B}^H \mathbf{Q}_{B(r)}^{-1} \bar{\mathbf{a}}_1}{\sigma_{s(r+1)}^{-2} + \mathbf{a}_{r+1}^H \mathbf{B}^H \mathbf{Q}_{B(r)}^{-1} \mathbf{B} \mathbf{a}_{r+1}} \bar{\mathbf{a}}_1^H \mathbf{Q}_{B(r)}^{-1} \mathbf{Q}_{B(r)}^{-1} \mathbf{B} \mathbf{a}_{r+1} \right) \end{aligned} \quad (\text{B17})$$

according to (B5). Again, utilizing the relationship of (B8), Eq. (B17) can be approximated to

$$\left\| \mathbf{Q}_{B(r+1)}^{-1} \bar{\mathbf{a}}_1 \right\|^2 \approx \left\| \mathbf{Q}_{B(r)}^{-1} \bar{\mathbf{a}}_1 \right\|^2. \quad (\text{B18})$$

Substituting (B18) and (B9) into (B16) and utilizing (B3) yields

$$P_{n,B(r+1)} \approx \sigma_n^2 \frac{\left\| \mathbf{Q}_{B(r)}^{-1} \bar{\mathbf{a}}_1 \right\|^2}{\left(\bar{\mathbf{a}}_1^H \mathbf{Q}_{B(r)}^{-1} \bar{\mathbf{a}}_1 \right)^2} \approx \sigma_n^2 \frac{\bar{\mathbf{a}}_1^H (\mathbf{B}\mathbf{B}^H)^{-1} (\mathbf{B}\mathbf{B}^H)^{-1} \bar{\mathbf{a}}_1}{\left[\bar{\mathbf{a}}_1^H (\mathbf{B}\mathbf{B}^H)^{-1} \bar{\mathbf{a}}_1 \right]^2}. \quad (\text{B19})$$

From the $P_{i,B}$ in (B15) and $P_{n,B}$ in (B19), we have $SINR_B$ for $q = r + 1$ given by

$$SINR_{B(r+1)} \approx \frac{\sigma_{s1}^2}{\sum_{k=2}^{r+1} \frac{\sigma_{sk}^2 \sigma_n^4 \bar{\mathbf{a}}_k^H (\mathbf{B}\mathbf{B}^H)^{-1} \bar{\mathbf{a}}_k |d_{1k,B}|^2}{\bar{\mathbf{a}}_1^H (\mathbf{B}\mathbf{B}^H)^{-1} \bar{\mathbf{a}}_1 [\sigma_n^2 + |\gamma_k|^2 \sigma_{sk}^2 \bar{\mathbf{a}}_k^H (\mathbf{B}\mathbf{B}^H)^{-1} \bar{\mathbf{a}}_k]}^2 + \sigma_n^2 \frac{\bar{\mathbf{a}}_1^H (\mathbf{B}\mathbf{B}^H)^{-1} (\mathbf{B}\mathbf{B}^H)^{-1} \bar{\mathbf{a}}_1}{\left[\bar{\mathbf{a}}_1^H (\mathbf{B}\mathbf{B}^H)^{-1} \bar{\mathbf{a}}_1 \right]^2}}, \quad (\text{B20})$$

which is the same as (69) with q replaced by $r + 1$. Therefore, it is proved by mathematical induction that the approximated $SINR_B$ in

(69) is valid for $2 \leq q < N$. As we discussed in Appendix A, the proposed formula in (69) may also be more inaccurate for greater q due to error propagation. However, our experiment in Section 5 shows that the errors are acceptable even if q approaches the number p of array elements. Especially, the approximated errors are tiny for small q/p .

APPENDIX C.

Define $F(t) \equiv f(t+1) - f(t) = \Delta f(t)$. Then we have [21]

$$\sum_{t=1}^{p-2} F(t) = f(p-1) - f(1). \tag{C1}$$

From (73) and (C1), we can let

$$F(t) = (p-t-1)(p-t)(p-t+1) \cos(t\rho_k), \tag{C2}$$

where $\rho_k \equiv \varphi_k - \varphi_1$. The corresponding $f(t)$ can be found as follows:

$$f(t) = \Delta^{-1} F(t), \tag{C3}$$

where the operation “ Δ^{-1} ” is given by [22]. Some common formulas of Δ^{-1} about trigonometry are given as follows [22]:

$$\begin{aligned} \Delta^{-1} \cos(at+b) &= \frac{\sin\left(at+b-\frac{a}{2}\right)}{2 \sin \frac{a}{2}} + C \\ \text{and } \Delta^{-1} \sin(at+b) &= \frac{-\cos\left(at+b-\frac{a}{2}\right)}{2 \sin \frac{a}{2}} + C, \end{aligned} \tag{C4}$$

where C is a constant. Utilizing “summation by parts” [22] and (C4), we have

$$\begin{aligned} &\Delta^{-1} (p-t-1)(p-t)(p-t+1) \cos(\rho_k t) \\ &= \frac{1}{2 \sin \frac{\rho_k}{2}} (p-t-1)(p-t)(p-t+1) \sin\left(\rho_k t - \frac{\rho_k}{2}\right) \\ &\quad + \frac{3}{2 \sin \frac{\rho_k}{2}} \Delta^{-1} (p-t-1)(p-t) \sin\left(\rho_k t + \frac{\rho_k}{2}\right) + C_1. \end{aligned} \tag{C5}$$

Similarly, we have

$$\begin{aligned} &\Delta^{-1} (p-t-1)(p-t) \sin\left(\rho_k t + \frac{\rho_k}{2}\right) \\ &= \frac{-1}{2 \sin \frac{\rho_k}{2}} (p-t-1)(p-t) \cos(\rho_k t) \\ &\quad - \frac{1}{\sin \frac{\rho_k}{2}} \Delta^{-1} (p-t-1) \cos(\rho_k t + \rho_k) + C_2 \end{aligned} \tag{C6}$$

and

$$\begin{aligned} & \Delta^{-1} (p - t - 1) \cos (\rho_k t + \rho_k) \\ &= \frac{1}{2 \sin \frac{\rho_k}{2}} (p - t - 1) \sin \left(\rho_k t + \frac{\rho_k}{2} \right) - \frac{1}{4 \sin^2 \frac{\rho_k}{2}} \cos (\rho_k t + \rho_k) + C_3. \end{aligned} \quad (\text{C7})$$

Substituting (C7) into (C6) yields

$$\begin{aligned} & \Delta^{-1} (p - t - 1) (p - t) \sin \left(\rho_k t + \frac{\rho_k}{2} \right) \\ &= \frac{-1}{2 \sin \frac{\rho_k}{2}} (p - t - 1) (p - t) \cos (\rho_k t) + \frac{1}{4 \sin^3 \frac{\rho_k}{2}} \cos (\rho_k t + \rho_k) \\ & \quad - \frac{1}{2 \sin^2 \frac{\rho_k}{2}} (p - t - 1) \sin \left(\rho_k t + \frac{\rho_k}{2} \right) + C_4. \end{aligned} \quad (\text{C8})$$

Then substituting (C8) into (C5), we obtain the function $f(t)$ as follows:

$$\begin{aligned} & \Delta^{-1} (p - t - 1) (p - t) (p - t + 1) \cos (\rho_k t) \\ &= \frac{1}{2 \sin \frac{\rho_k}{2}} (p - t - 1) (p - t) (p - t + 1) \sin \left(\rho_k t - \frac{\rho_k}{2} \right) \\ & \quad - \frac{3}{4 \sin^2 \frac{\rho_k}{2}} (p - t - 1) (p - t) \cos (\rho_k t) \\ & \quad - \frac{3}{4 \sin^3 \frac{\rho_k}{2}} (p - t - 1) \sin \left(\rho_k t + \frac{\rho_k}{2} \right) + \frac{3}{8 \sin^4 \frac{\rho_k}{2}} \cos (\rho_k t + \rho_k) + C_5 \\ &= f(t). \end{aligned} \quad (\text{C9})$$

From (C1)–(C3) and (C9), it is easy to find that

$$\begin{aligned} & \sum_{t=1}^{p-2} (p - t - 1) (p - t) (p - t + 1) \cos (t \rho_k) \\ &= \frac{3}{8 \sin^4 \frac{\rho_k}{2}} [\cos (p \rho_k) - 1] + \frac{3}{4 \sin^2 \frac{\rho_k}{2}} p^2 - \frac{1}{2} p (p^2 - 1). \end{aligned} \quad (\text{C10})$$

As a result, (74) can be obtained by substituting (C10) and $\rho_k = \varphi_k - \varphi_1$ into (73).

APPENDIX D.

Following the definition of $d_{ij,B}$, $|d_{1k,B}|^2$ can be expressed by

$$|d_{1k,B}|^2 = \frac{\left| \bar{\mathbf{a}}_1^H (\mathbf{B}\mathbf{B}^H)^{-1} \bar{\mathbf{a}}_k \right|^2}{\bar{\mathbf{a}}_1^H (\mathbf{B}\mathbf{B}^H)^{-1} \bar{\mathbf{a}}_1 \bar{\mathbf{a}}_k^H (\mathbf{B}\mathbf{B}^H)^{-1} \bar{\mathbf{a}}_k}. \quad (\text{D1})$$

The unknown term $\overline{\mathbf{a}}_1^H (\mathbf{B}\mathbf{B}^H)^{-1} \overline{\mathbf{a}}_k$ can be derived with some algebra manipulations and Calculus of Finite Differences [21, 22], respectively. The results are given as follows:

$$\begin{aligned} \text{Re} \left[\overline{\mathbf{a}}_1^H (\mathbf{B}\mathbf{B}^H)^{-1} \overline{\mathbf{a}}_k \right] &= \frac{p-1}{4} + \frac{1}{8\sin^3 \frac{\rho_k}{2}} \sin \left[\left(p - \frac{1}{2} \right) \rho_k \right] \\ &\quad - \frac{1}{8\sin^2 \frac{\rho_k}{2}} \{ p - 2 + (p+1) \cos [(p-1) \rho_k] \}, \quad (\text{D2}) \end{aligned}$$

$$\begin{aligned} \text{Im} \left[\overline{\mathbf{a}}_1^H (\mathbf{B}\mathbf{B}^H)^{-1} \overline{\mathbf{a}}_k \right] &= \frac{p-1}{4 \sin \frac{\rho_k}{2}} \cos \left(\frac{\rho_k}{2} \right) - \frac{p+1}{8\sin^2 \frac{\rho_k}{2}} \sin [(p-1)\rho_k] \\ &\quad + \frac{1}{8\sin^3 \frac{\rho_k}{2}} \left\{ \cos \left(\frac{\rho_k}{2} \right) - \cos \left[\left(p - \frac{1}{2} \right) \rho_k \right] \right\}, \quad (\text{D3}) \end{aligned}$$

where $\text{Im}\{x\}$ denotes the imaginary part of x and $\rho_k = \varphi_k - \varphi_1$ is the same as that in Appendix C. Based on (D2) and (D3), we obtain

$$\begin{aligned} & \left| \overline{\mathbf{a}}_1^H (\mathbf{B}\mathbf{B}^H)^{-1} \overline{\mathbf{a}}_k \right|^2 \\ &= \left\{ \text{Re} \left[\overline{\mathbf{a}}_1^H (\mathbf{B}\mathbf{B}^H)^{-1} \overline{\mathbf{a}}_k \right] \right\}^2 + \left\{ \text{Im} \left[\overline{\mathbf{a}}_1^H (\mathbf{B}\mathbf{B}^H)^{-1} \overline{\mathbf{a}}_k \right] \right\}^2 \\ &= \frac{\left\{ \begin{aligned} & p^2 + 1 + (p^2 - 1) [\cos(p\rho_k) - \cos \rho_k] \\ & - (p-1)^2 \cos(p\rho_k) \cos \rho_k - 2p \cos[(p-1)\rho_k] \end{aligned} \right\}}{8(1 - \cos \rho_k)^3}. \quad (\text{D4}) \end{aligned}$$

Substituting (74), (75), and (D4) into (D1) yields

$$|d_{1k,B}|^2 = \frac{3 \left\{ \begin{aligned} & p^2(1 - \cos \rho_k) + 1 - \cos(p\rho_k) + \cos \rho_k [1 - \cos(p\rho_k)] \\ & + p^2 \cos(p\rho_k)(1 - \cos \rho_k) - 2p \sin(p\rho_k) \sin(\rho_k) \end{aligned} \right\}}{(p^2 - 1)(1 - \cos \rho_k) [p^2(1 - \cos \rho_k) + \cos(p\rho_k) - 1]}. \quad (\text{D5})$$

It follows from (76) that the assumption $|d_{1k}|^2 \ll 1$ for a ULA is equivalent to $1 - \cos(p\rho_k) \ll p^2(1 - \cos \rho_k)$. Thus, $|d_{1k,B}|^2$ can be approximated as

$$\begin{aligned} & |d_{1k,B}|^2 \\ & \approx \frac{3[p^2(1 - \cos \rho_k) + p^2 \cos(p\rho_k)(1 - \cos \rho_k) - 2p \sin(p\rho_k) \sin(\rho_k)]}{p^2(p^2 - 1)(1 - \cos \rho_k)^2} \\ & = \frac{3[1 + \cos(p\rho_k)]}{(p^2 - 1)(1 - \cos \rho_k)} - \frac{6 \sin(p\rho_k) \sin(\rho_k)}{p(p^2 - 1)(1 - \cos \rho_k)^2} \quad (\text{D6}) \end{aligned}$$

when $|d_{1k}|^2 \ll 1$ holds. It can be seen from (D6) that $|d_{1k,B}|^2$ is in general much less than 1 for a moderate number of array elements.

ACKNOWLEDGMENT

This work was supported by the National Science Council of TAIWAN under Grants NSC97-2221-E002-174-MY3 and NSC100-2221-E002-200-MY3.

REFERENCES

1. Wax, M. and Y. Anu, "Performance analysis of the minimum variance beamformer," *IEEE Trans. Signal Process.*, Vol. 44, No. 4, 928–937, Apr. 1996.
2. Chang, L. and C.-C. Yeh, "Performance of DMI and eigenspace-based beamformers," *IEEE Trans. Antennas Propag.*, Vol. 40, No. 11, 1336–1347, Nov. 1992.
3. Reed, I. S., J. D. Mallett, and L. E. Brennan, "Rapid convergence rate in adaptive arrays," *IEEE Trans. Aerosp. Electron. Syst.*, Vol. 10, No. 6, 853–863, Nov. 1974.
4. Widrow, B., K. M. Duvall, R. P. Gooch, and W. C. Newman, "Signal cancellation phenomena in adaptive antennas: Causes and cures," *IEEE Trans. Antennas Propag.*, Vol. 30, No. 3, 469–478, May 1982.
5. Haimovich, A. M. and Y. Bar-Ness, "An eigenanalysis interference canceler," *IEEE Trans. Signal Process.*, Vol. 39, No. 1, 76–84, Jan. 1991.
6. Choi, Y.-H., "Performance improvement of adaptive arrays with signal blocking," *IEICE Trans. Comm.*, Vol. E86-B, No. 8, 2553–2557, Aug. 2003.
7. Choi, Y.-H., "Signal-blocking-based adaptive beamformer with simple direction error correction," *Electron. Lett.*, Vol. 40, No. 8, 463–464, Apr. 2004.
8. Lee, J.-H. and C.-C. Lee, "Analysis of the performance and sensitivity of an eigenspace-based interference canceler," *IEEE Trans. Antennas Propag.*, Vol. 48, No. 5, 826–835, May 2000.
9. Lee, J.-H. and Y.-H. Lee, "Two-dimensional adaptive array beamforming with multiple beam constraints using a generalized sidelobe canceler," *IEEE Trans. Signal Process.*, Vol. 53, No. 9, 3517–3529, Sep. 2005.
10. Choi, Y.-H., "Duvall-structure-based fast adaptive beamforming for coherent interference cancellation," *IEEE Signal Process. Lett.*, Vol. 14, No. 10, 739–741, Oct. 2007.
11. Yu, L., W. Liu, and R. Langley, "SINR analysis of the subtraction-

- based SMI beamformer,” *IEEE Trans. Signal Process.*, Vol. 58, No. 11, 5926–5932, Nov. 2010.
12. Steinhardt, A. O., “The PDF of adaptive beamforming weights,” *IEEE Trans. Signal Process.*, Vol. 39, No. 5, 1232–1235, May 1991.
 13. Richmond, C. D., “PDF’s confidence regions, and relevant statistics for a class of sample covariance-based array processors,” *IEEE Trans. Signal Process.*, Vol. 44, No. 7, 1779–1793, Jul. 1996.
 14. Frost, O. L., “An algorithm for linearly constrained adaptive array processing,” *Proc. IEEE*, Vol. 60, No. 8, 926–935, Aug. 1972.
 15. Li, R., X. Zhao, and X. W. Shi, “Derivative constrained robust LCMV beamforming algorithm,” *Progress In Electromagnetics Research C*, Vol. 4, 43–52, 2008.
 16. Li, Y., Y. J. Gu, Z. G. Shi, and K. S. Chen, “Robust adaptive beamforming based on particle filter with noise unknown,” *Progress In Electromagnetics Research*, Vol. 90, 151–169, 2009.
 17. Griffiths, L. J. and C. W. Jim, “An alternative approach to linearly constrained adaptive beamforming,” *IEEE Trans. Antennas Propag.*, Vol. 30, No. 1, 27–34, Jan. 1982.
 18. Trim, D., *Calculus for Engineers*, Prentice Hall, Toronto, 2008.
 19. Sominskii, I. S., *The Method of Mathematical Induction*, Pergamon, London, 1961.
 20. Larson, R., B. H. Edwards, and D. C. Falvo, *Elementary Linear Algebra*, Brooks Code, CA, 2009.
 21. Miller, K. S. and J. B. Walsh, *Elementary and Advanced Trigonometry*, 212–215, Harper & Brothers, New York, 1962.
 22. Jordan, C., *Calculus of Finite Differences*, 100–107, Chelsea, New York, 1947.